Natural-product-inspired design and synthesis of two series of compounds active against Trypanosoma cruzi: Insights into structure–activity relationship, toxicity, and mechanism of action

Rafael da Rosa, Bibiana Paula Dambrós, Milene Höehr de Moraes, Lucie Grand, Maïwenn Jacolot, Florence Popowycz, Mario Steindel, Eloir Paulo Schenkel, Lílian Sibelle Campos Bernardes

Version of Record: https://www.sciencedirect.com/science/article/pii/S0045206821008701
Manuscript_15ec10271f8e441628c22f77434ece3a

Natural-product-inspired design and synthesis of two series of compounds active against *Trypanosoma cruzi:* Insights into structure–activity relationship, toxicity, and mechanism of action

Rafael da Rosa[1,3*], Bibiana Paula Dambrós[2], Milene Höehr de Moraes[2], Lucie Grand[3], Maïwenn Jacolot[3], Florence Popowycz[3], Mario Steindel[2], Eloir Paulo Schenkel[1], Lílian Sibelle Campos Bernardes[1*]

[1]Laboratório de Química Farmacêutica Medicinal, Programa de Pós-Graduação em Farmácia, CCS, Universidade Federal de Santa Catarina. Campus Universitário, 88040900, Florianópolis, Brasil.

[2]Laboratório de Protozoologia, CCB, Universidade Federal de Santa Catarina. Campus Universitário, 88040900, Florianópolis, Brasil.

[3]Université de Lyon, INSA Lyon, Université Lyon 1, CNRS, CPE Lyon, UMR 5246, ICBMS. 1 rue Victor Grignard, 69621, Villeurbanne Cedex, France.

*Corresponding authors: l.bernardes@ufsc.br; rafael.rosa@posgrad.ufsc.br

Abstract

Chemical scaffolds of natural products have historically been sources of inspiration for the development of novel molecules of biological relevance, including hit and lead compounds. To identify new compounds active against *Trypanosoma cruzi*, we designed and synthesized 46 synthetic derivatives based on the structure of two classes of natural products: tetrahydrofuran lignans (Series 1) and oxazole alkaloids (Series 2). Compounds were screened in vitro using a cellular model of *T. cruzi* infection. In the first series of compounds, 11 derivatives of hit compound **5** (EC_{50} = 1.1 µM) were found to be active; the most potent (**7**, **8**, and **13**) had EC_{50} values of 5.1–34.2 µM. In the second series, 17 analogs were found active at 50 µM; the most potent compounds (**47**, **49**, **59**, and **63**) showed EC_{50} values of 24.2–49.1 µM. Active compounds were assessed for selectivity, hemocompatibility, synergistic potential, effects on mitochondrial membrane potential, and inhibitory effect on trypanothione reductase. All active compounds showed low toxicity against uninfected THP-1 cells and human erythrocytes. The potency of compounds **5** and **8** increased steadily in combination with benznidazole, indicating a synergistic effect. Furthermore, compounds **8**, **47**, **49**, **59**, and **63** inhibited parasitic mitochondria in a dose-dependent manner. Although increased reactive oxygen species levels might be involved in the mitochondrial effects caused by compounds, the results indicate that the mechanism of action is not dependent on trypanothione reductase inhibition. In silico calculation of chemical descriptors and principal component analysis showed that the active compounds share common chemical features with other trypanocidal molecules and are predicted to have a good ADMET profile. Overall, the results suggest that the compounds are important candidates to be further studied for their potential against *T. cruzi*.

Keywords: *T. cruzi*, mitochondrial dysfunction, isoxazole, oxazole, antiparasitic, neglected tropical diseases, natural products.

1. Introduction

Trypanosoma cruzi, the causative agent of Chagas disease, is a hemoflagellate protozoan parasite first described by Carlos Chagas in 1909. Its complex life cycle involves multiple distinct morphological stages in both mammalian hosts and triatomine vectors. Not long after this discovery, the human disease caused by *T. cruzi* was identified and named Chagas disease [1]. The acute phase of Chagas disease occurs right after infection and presents with unspecific symptoms such as fever and malaise. This stage is characterized by high parasitemia, which facilitates diagnosis. Following the acute stage, the disease enters an indeterminate stage where the amastigote form of *T. cruzi* is found intracellularly in different tissues. Although silent, the presence of the parasite leads to chronic inflammation and tissue damage. These effects ultimately result in the potentially fatal complications seen during the chronic stage of the disease, such as cardiac and gastrointestinal dysfunction [2,3]. Society has experienced important advances in science and medicine more than a century since the first reports, but Chagas disease remains a public health concern, especially in Latin America [4].

The nitroheterocyclic drugs benznidazole and nifurtimox are used for the treatment of Chagas disease. However, both drugs have a high incidence of side effects, causing a significant number of patients to discontinue treatment [5–8]. In some cases, parasite resistance greatly affects the efficacy of trypanocidal drugs [9,10]. Yet another challenge is that benznidazole and nifurtimox are not effective in addressing Chagas disease during its indeterminate and chronic stages, leaving millions of patients at risk of facing the life-threatening consequences of the infection [11]. Over the last years, few clinical trials have been conducted to assess the efficacy of other drugs in the treatment of Chagas disease. Patients treated with posaconazole had no long-term benefit in comparison with those treated with benznidazole [12]. Treatment with E1224 (prodrug of ravuconazole) was able to reduce the parasite load to undetectable levels by the end of treatment, but a follow-up assessment conducted months later revealed that the infection was active again [13–15]. The nitroheterocyclic drug fexinidazole has been recently approved for the treatment of sleeping sickness, caused by another species of the genus *Trypanosoma*, *T. brucei gambiense*; the results of an ongoing trial in patients with Chagas disease are expected shortly [16,17].

The need for new chemical entities that are active against *T. cruzi* is clear. Chemical compounds obtained from natural sources have long been explored for their medicinal properties [18–21], and this situation is no different when it comes to the chemical space occupied by antitrypanosomal molecules. Numerous alkaloids, quinones, lignans, and terpenoids have been described as active against *T. cruzi* strains [22]. Some challenges, however, limit the translation of natural products to marketable drugs. Most limitations are

related to the large-scale availability of the natural source, concerns about biodiversity exploration, or the need for labor-intensive techniques for isolation of target metabolites. Additionally, the fine balance between biological activity and pharmaceutical properties related to chemical structure, such as solubility, bioavailability, and metabolic stability, might not be easily encountered in unmodified natural products [23,24].

The synthesis of natural product analogs has been widely used to overcome these limitations and facilitate the study of the structure–activity relationship of natural scaffolds [25,26]. Up to one-third of FDA-approved drugs are natural product derivatives, including compounds obtained either by semi- or total synthesis or inspired by a natural product or a natural pharmacophore moiety. By contrast, unaltered natural products account for less than 4% of approved drugs [27]. Recent review articles have shown that natural-product-inspired design and synthesis have been applied to obtain derivatives active against *T. cruzi*. In multiple cases, the potency of derivatives against different strains and life stages of the parasite is comparable to that of benznidazole [28,29]. Such findings demonstrate that natural scaffolds can be an important starting point for the design of novel trypanocidal hits.

In this study, we report the use of two classes of natural products as potential starting points in the development of new molecules that are active against *T. cruzi*. The biological activity of tetrahydrofuran lignans against *T. cruzi* is well documented, and multiple derivatives have been described in the literature, including by our research group. On the basis of such data, we further explored the potential of the lignan scaffold and investigated whether natural products that share similar chemical features could also act against *T. cruzi*. Within the latter category, we proposed derivatives of balsoxine-like oxazole alkaloids. Although the natural alkaloids themselves were found not active against *T. cruzi*, derivatives modified to contain a bisheterocyclic scaffold showed improved biological potential. After an initial screening, the active compounds were further tested to gain insight into their toxicity (selectivity over uninfected cells, hemotoxicity, and effects on *T. cruzi* plasmatic membrane) and mechanism of action (mitochondrial effects and trypanothione reductase inhibition). The potential of the most potent derivative to act synergistically with benznidazole is also reported.

2. Results and Discussion

2.1. New compounds based on the scaffold of natural tetrahydrofuran lignans: Rationale, synthesis, and evaluation against T. cruzi amastigotes

In plants, the condensation of two phenylpropanoids units leads to a class of secondary metabolites named lignans. Depending on which position of the phenylpropanoid unit the condensation takes place, more than twenty different scaffolds might be formed [30]. Tetrahydrofuran lignans (such as compounds **1**–**3**) are in the largest group of lignans

described with trypanocidal activity [31–33]. Their *in vitro* potencies (EC_{50}) range from 2.2 to 58.7 µM, however, the low yield in which they are isolated from plants compromises their developmentability as lead compounds (Fig.1). Due to the presence of multiple chiral centers, the total synthesis of tetrahydrofuran lignans is also complicated, requiring many synthetic steps, and affording the final compounds in low global yields [34–36].

In an attempt of overcoming these limitations, the scaffold of the tetrahydrofuran lignans has been used as inspiration for designing new derivatives through more accessible synthetic routes. This approach also leads to chemically diverse derivatives, which might contribute to study structure-activity relationships and improving physicochemical properties, such as solubility. Examples of analogues include, dihydrofuran-[37], 1,4-diketo-1,4-diphenylbutan-[38], furan-[39], isoxazole-[40], triazole-[41] and bisheterocyclic-containing molecules [42].

In previous work on this topic, our research group described a new series of 3,5-disubstituted isoxazole derivatives active against *T. cruzi* [40]. From the first set of analogs, the *hit* compound 3-(3,4-methylenedioxyphenyl)-5-(4-hydroxymethylphenyl)isoxazole (Compound **4**, EC_{50} = 5.1 µM) was identified. Compound **4** was then derivatized and we could identify that the *p*-phenyl substituent was necessary for increasing potency. Moreover, the replacement of the 4-hydroxymethyl group by apolar substituents such as 4–methyl and 4–chloromethyl was responsible for a further increase in potency. The 4–chloromethyl bearing compound **5** was the most active and selective in that series, with EC_{50} = 1,1 µM and selectivity index (SI) = 165 (Fig. 1).

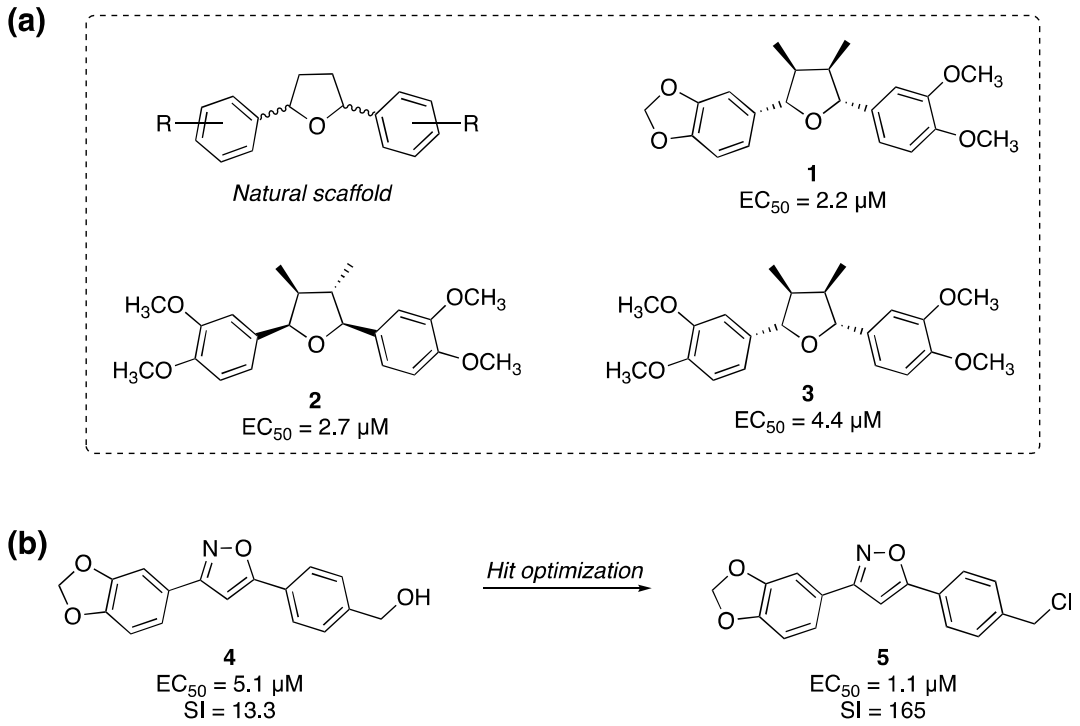

Fig. 1. (a) Structure of a few natural tetrahydrofuran lignans **1**–**3** with remarkable activity against *T. cruzi* (trypomastigotes, Y strain). The natural scaffold, common to other compounds, comprises a central tetrahydrofuran ring linked to two substituted aryl rings. (b) Isoxazole-containing analogues **4**–**5** of the natural lignans active against *T. cruzi* (amastigotes, Tulahuen strain).

In this work, aiming to deepen our understanding of the structure-activity relationship, we have synthesized derivatives of compound **5**. Similar to the synthesis of compound **5** using a halosulfoxide reagent, a compound containing the 4-bromomethyl substituent (Compound **6**) could be obtained from the reaction of compound **4** with thionylbromide. Compound **4** also was the starting material for the synthesis of compound **7** using DeoxoFluor® as a nucleophilic fluorinating reagent. Multiple unidentified side-products were formed during this reaction and compound **7** could only be obtained with a low yield after several attempts. Lastly, a compound containing a substituent 4-iodomethyl (Compound **8**) was obtained *via* the reaction of compound **5** with potassium iodide (Fig. 2).

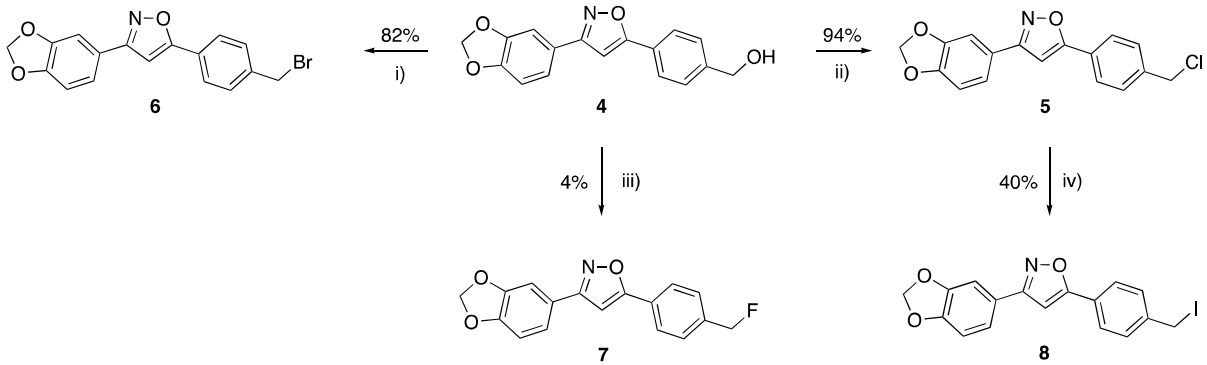

Fig. 2. Yields are represented on top or to the left of arrows. i) $SOBr_2$ (3.0 eq), CH_2Cl_2 (0.85 M), Ar, r.t., 1h. ii) $SOCl_2$ (3.0 eq), CH_2Cl_2 (0.85 M), Ar, r.t., 1 h. iii) DeoxoFluor (1.05 eq), CH_2Cl_2 (0.85 M), Ar, 0 °C, 20 h. iv) Potassium iodide (1.2 eq), acetone (0.8 M), r.t, 20 h.

The replacement of chlorine by other halogens modifies logP, surface area, orbital energy, and other properties that could modulate either the activity against *T. cruzi* or the toxicity of the compounds. After the synthesis, the biological evaluation was performed using a colorimetric assay with amastigotes of *T. cruzi* (Tulahuen strain) genetically modified to express the enzyme β-galactosidase. The results revealed that compounds **7** and **8** also are active against *T. cruzi*. The potency of these compounds is lower than that of compound **5**. However, they are still comparable to benznidazole regarding potency. Compound **6** has low activity against the parasite, causing the death of only 20% of the parasites at the concentration of 50 μM. Therefore, the compound was not evaluated in multiple concentrations for EC_{50} determination.

Looking at cytotoxicity data, compounds bearing more electronegative atoms at the benzylic position are more toxic to THP-1 cells (Table 1). This was expected due to lower LUMO energy at the benzylic carbon, which would facilitate the attack of cellular nucleophiles, such as DNA and some amino acid residues. Combining both biological outputs, compound **5** remains the most potent and selective compound against *T. cruzi* among the halogenated series.

Table 1. Effect of the treatment (72 h) with compounds **5**–**8** in *T. cruzi* amastigotes (EC_{50}) and THP-1 cells (CC_{50}).

ID	Maximum activity (%)[a]	EC_{50} *T. cruzi* (µM)	CC_{50} THP-1 (µM)	SI
5	92.7 (±2.3)	1.1 (±0.4)	181.8 (±25.9)	165
6	20.0 (±2.8)	–	–	–
7	79.3 (±3.3)	5.1 (±1.1)	361.4 (±63.9)	70.8
8	89.0 (±2.0)	9.8 (±1.4)	31.8 (±3.7)	3.2
Bzn	96.6 (±1.6)	10.2 (±0.8)	>500	>49

The results represent (average ± SD) of two independent experiments in triplicate. [a]Percentage of parasite death after the treatment with 50 µM of the compounds. Compounds that led to more than 45% of parasite death were evaluated in different concentration for EC_{50} and CC_{50} determination. SI = selectivity index, CC_{50}/EC_{50}

Having this in mind, we planned new derivatives in which the isoxazole ring in the central region of the molecule was replaced by other linkers either acyclic or heterocyclic. A total of eleven derivatives could be obtained containing ester, amide, ether, amine, α,β-unsaturated ketone, triazole, isoxazoline, oxazole and oxadiazole bridges between the two aryl rings present in compound **5**.

All final compounds could be synthesized from simple building blocks using classical synthetic methodologies. For synthesizing compounds **10** and **11**, 4-chloromethylbenzoic acid **9** was coupled to piperonyl-alcohol or amine. The benzoic acid derivative was activated *via* an acyl chloride intermediate or using carbonyldiimidazole, respectively. Carbonyldiimidazole was also used for the coupling of **9** and 3,4-methylenedioxyamidoxime, for the preparation of the intermediate **12** used for the synthesis of the 1,2,4-oxadiazole derivative **13** (Fig. 3).

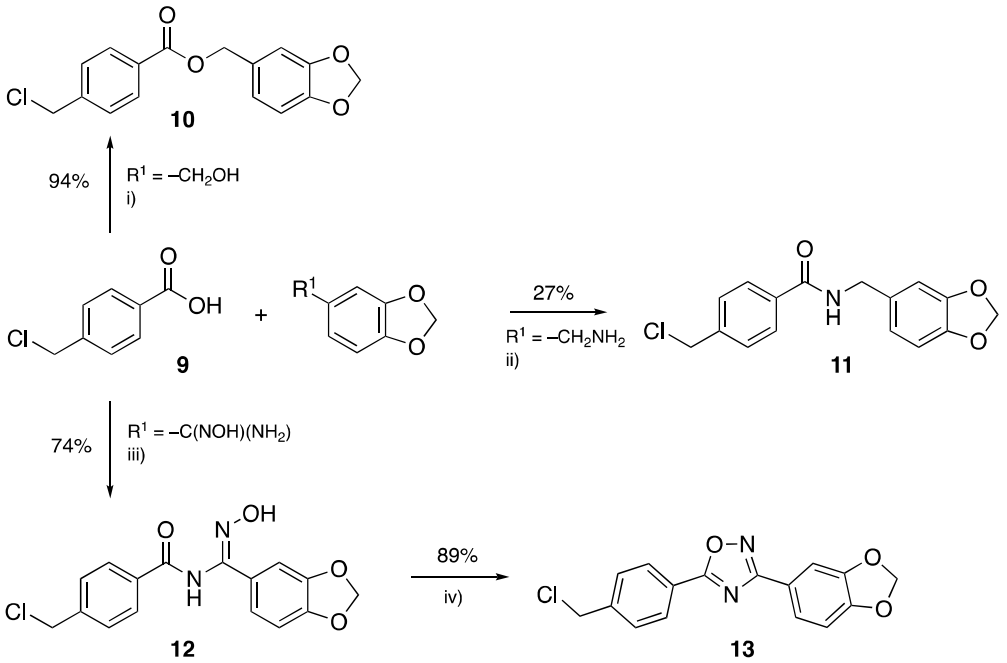

Fig. 3. Yields are represented on top or to the left of arrows. i) $SOCl_2$ (3.0 eq), CH_2Cl_2 (0.15 M), Ar, reflux, 1 h, then Et_3N, piperonyl alcohol (1.0 eq), CH_2Cl_2, reflux, 2 h. ii) CDI (1.1 eq), piperonylamine (1.1 eq after 30 min), THF (0.15 M), r.t., 20 h. iii) CDI (2.0 eq), DMF (0.3 M), r.t., overnight. iv) DMF (0.08 M), 80 °C, 4h.

4-Chloromethylbenzaldehyde **15** was the starting material for the synthesis of compounds **16** and **17**. The building block was prepared through the Jones oxidation of 4-chloromethylbenzylalcohol **14** and reacted *via* reductive amination with piperonyl-amine or via Claisen-Schmidit condensation with piperonyl-acetophenone to form compounds **16** and **17**, respectively (Fig. 4).

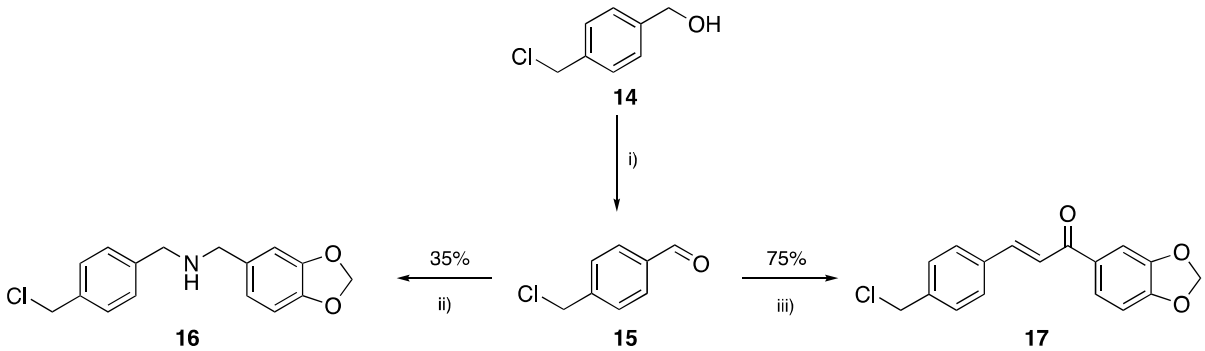

Fig. 4. Yields are represented on top of arrows. i) Jones reagent 6 N (1.5 eq dropwise), acetone (0.3 M), 0 °C to r.t., 15 min. ii) piperonylamine (1 eq), CH_2Cl_2 (0.15 M), $NaBH_4$ (1.0 eq), MeOH (1 drop), r.t. iii) 3,4-methylenedioxyacetophenone (1.0 eq), NaOH/MeOH 10% (0.6 M), r.t. 4 h.

Compounds **20** and **23** could be obtained through 1,3-dipolar cycloaddition using piperonylnitrile oxide **18** and piperonylazide **21** as 1,3-dipoles. 4-Vinylbenzyl alcohol and 4-ethynylbenzyl alcohol were used as dipolarophiles for obtaining the hydroxy-derivatives **19**

and **22** that ultimately led to compounds **20** and **23** respectively. Finally, compound **26** was obtained via the arylation of piperonyl-5-oxazole **24** using 4-iodo-benzylalcohol as coupling partner. The synthetic routes are depicted in Fig. 5.

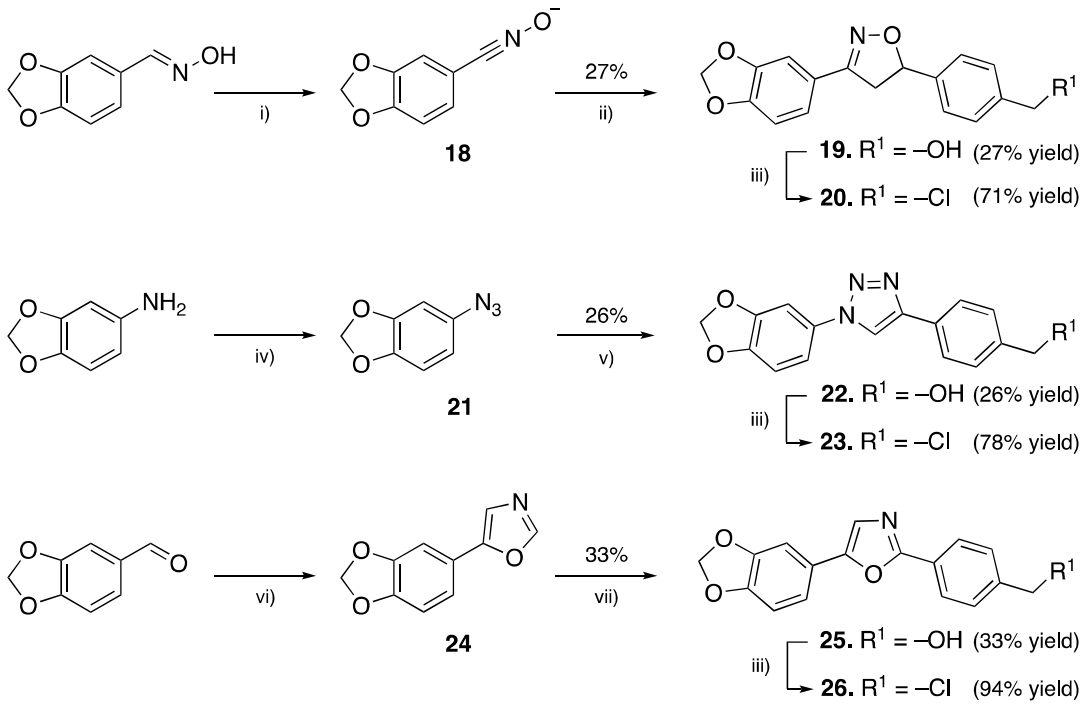

Fig. 5. Yields are represented on top of arrows. i) NCS (1.1 eq), DMF (0.3 M), r.t. ii) 4-ethynylbenzylalcohol (1.1 eq), $NaHCO_3$ (4.0 eq), copper(ii) sulfate (2 mol%), sodium ascorbate (10 mol%), H_2O:tBuOH (0.15 M), r.t., 2 h. iii) $SOCl_2$ (3 eq), CH_2Cl_2 (0.15 M), r.t., 1 h. iv) $NaNO_3$ (1.5 eq), HCl 6 M (0.18 M), NaN_3 (4.0 eq), 0 °C to r.t., 2 h. v) 4-vinylbenzylalcohol (1.1 eq), copper(ii) sulfate (2 mol%), sodium ascorbate (10 mol%), DMF (0.15 M), 70 °C MW, 10 min. vi) TosMIC (1 eq), K_2CO_3 (2 eq), MeOH (0.2 M), reflux, 2 h. vii) 4-iodobenzylalcohol (1.2 eq), K_2CO_3 (2 eq), CuI (1 eq), TPP (0.2 eq), DMF (0.3 M), 100 °C, 24 h.

After purification and chemical characterization (NMR and HRMS), the effect of the compounds on *T. cruzi* viability was assessed. The results are compiled in Table 2.

Table 2. Effect of the treatment (72 h) with compounds **10**–**13**, **16**, **17**, **19**, **20**, **22**, **23**, **25** and **26** in *T. cruzi* amastigotes (Tulahuen strain).

ID	Maximum activity (%)[a]	EC_{50} *T. cruzi* (µM)	SI
10	19.6 (±1.4)	–	–
11	NA	–	–
13	46.2 (±5.8)	34.2 (±1.8)	>29[b]
16	NA	–	–
17	17.0 (±0.8)	–	–
19	3.9 (±2.6)	–	–
20	16.8 (±6.6)	–	–
22	NA	–	–
23	9.1 (±1.9)	–	–
25	10.4 (±3.8)	–	–
26	3.1 (±0.3)	–	–
Bzn	85.6 (±2.5)	10.2 (±0.8)	>49

The results represent (average ± SD) of one experiment in triplicate. [a]Percentage of parasite death after the treatment with 50 µM of the compounds. NA = Not active [p >0.05 (ANOVA/Dunnet) in comparison with the negative control]. Bzn = Benznidazole. Compounds that led to more than 45% of parasite death were evaluated in different concentrations for EC_{50} and CC_{50} determination. [b]The treatment with 1 mM of the compound reduced cell viability by only 33.7%.

Most of the newly synthesized compounds were poorly active against *T. cruzi*, being capable of reducing parasite viability by a maximum of 20% at 50 µM. Compound **13** was the most active among the compounds evaluated. Therefore, the effect of multiple concentrations of compound **13** against infected cells was assessed to determine the EC_{50} (34.2 µM). The cytotoxicity of the compound in non-infected THP-1 cells is low, contributing to a high selectivity (SI >29).

The replacement of the isoxazole ring of compound **5** by other chemical moieties in the new compounds leads to changes in molecular shape and modifies properties that could affect interactions with a putative molecular target. We could observe that changes in the central region of the molecule are more detrimental to trypanocidal activity than changes in aromatic substituents (such as in compounds **4** and **6**–**8**). In compounds **19**–**20**, **22**–**23**, and **25**–**26**, we see a small difference in activity caused by the replacement of the 4-chloromethyl substituent by the 4-hydroxymethyl substituent. However, the activity is still lower than that observed for compounds **4** and **5**. As compound **13** was the only one described in Table 2 with significant activity, we could suggest that a central aromatic ring is indeed a requirement for activity against the parasite. However, the number and type of heteroatom in this ring play a role in

modulating activity. To date, the isoxazole ring seems to be the ideal choice in between the evaluated options.

2.2. New derivatives based on the scaffold of natural oxazole alkaloids: Rationale, synthesis, and evaluation against T. cruzi amastigotes

Oxazole-containing alkaloids have been isolated from marine and terrestrial organisms and described with multiple biological activities [43,44]. Among them, compounds containing the 2,5-diaryloxazole scaffold were obtained from different species of higher plants from the genera *Halfordia* and *Amyris* (Rutaceae). Texamine (**27**), texaline (**28**), balsoxine (**29**), halfordinol (**30**), and uguenenazole (**31**) are examples of compounds in the class (Fig. 2) [45–47]. These molecules differ among each other in the number and type of substituents in the aromatic ring and in the type of aromatic ring linked to position 2 of the oxazole ring. The C2-linked ring might be an aryl or heteroaryl ring depending on the specific compound. The scaffold similarity between balsoxine-like alkaloids, the tetrahydrofuran lignans, and their derivatives led us to contemplate whether these molecules could also be active against *T. cruzi*. The natural compounds have scarce reports of biological properties, except for the anti-mycobacterial properties of compound **28** and the lipolytic activity of compound **30** [48–50]. Synthetic derivatives possessing a similar scaffold were described with cytotoxic properties, and others also affected the viability of *Caenorhabditis elegans* or of multiple species in the genus *Trypanosoma, such as T. brucei, T. congolense,* and *T. evansi* [51–54].

In the previous section, we observed that the oxazole compounds **25** and **26** showed a weak activity against *T. cruzi*. To optimize both potency and chemical properties we undertook a more disruptive approach proposing a bisheterocyclic scaffold where one of the aryl rings linked to the oxazole core was replaced by a hydroxymethylfurfuryl moiety. A similar strategy has been previously applied to isoxazole derivatives and afforded a series of compounds with interesting biological profiles [42]. The presence of a hydroxymethyl group in the compounds also resembles active molecules such as the ones described herein earlier. Hence, the novel derivatives combine features of both natural and synthetic products with known trypanocidal properties (Fig. 6).

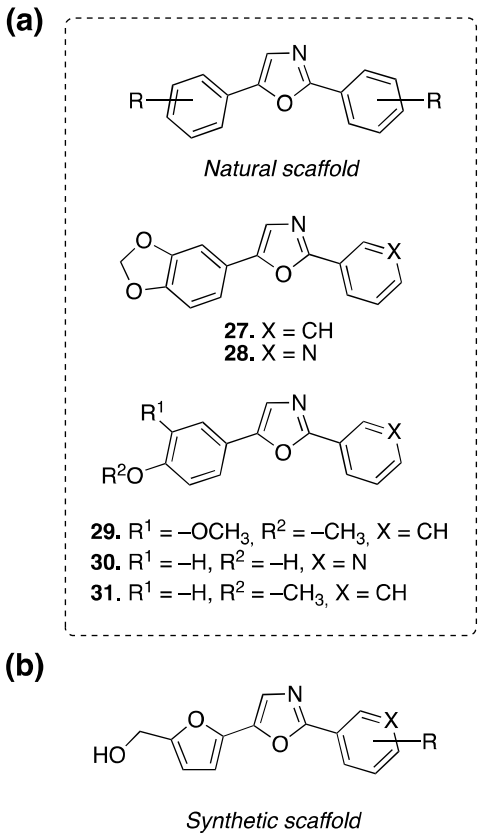

Fig. 6. (a) Structure of natural oxazole alkaloids **27**–**31** isolated from higher plants. The natural scaffold, common to other compounds, comprises a central oxazole ring linked to two substituted aryl rings. (b) Synthetic scaffold designed from combining the structure of oxazole alkaloids **27**–**31** and other trypanocidal compounds.

To obtain the final compounds, we used 5-hydroxymethylfurfural (5-HMF) as starting material in a two-step synthetic route, similar to that depicted in Fig. 5 (for the synthesis of compound **25**). To explore the chemical reactivity and contributing to the valorization of the bio-based building block 5-HMF, we put our efforts in optimizing the second step of the synthetic route. This step would be common to the synthesis of all derivatives and 5-HMF is proven to be a challenging substrate under some specific conditions [55,56]. After assessing multiple variables, the final synthetic route allowed us to obtain thirty-two derivatives **32**–**63**. We chose aromatic substituents in compounds to cover a range of different electronic, steric, and physicochemical properties. Overall, all of them could be obtained with fair to good yields of 20–85% (Fig. 7). The methodological details were made available by our research group elsewhere [57].

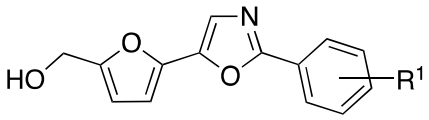

Scaffold A

32. R^1 = 4–OCH_3 I Yield = 72%
33. R^1 = 3–OCH_3 I Yield = 63%
34. R^1 = 2–OCH_3 I Yield = 71%
35. R^1 = 4–CH_3 I Yield = 85%
36. R^1 = 3–CH_3 I Yield = 53%
37. R^1 = 2–CH_3 I Yield = 69%
38. R^1 = 4–CF_3 I Yield = 69%
39. R^1 = 3–CF_3 I Yield = 70%
40. R^1 = 2–CF_3 I Yield = 29%
41. R^1 = 4–Cl I Yield = 56%
42. R^1 = 3–Cl I Yield = 83%
43. R^1 = 2–Cl I Yield = 83%
44. R^1 = 4–F I Yield = 67%
45. R^1 = 3–F I Yield = 82%
46. R^1 = 2–F I Yield = 51%
47. R^1 = 4–^{t}Bu I Yield = 71%
48. R^1 = 4–Ph I Yield = 58%
49. R^1 = 4–Br I Yield = 31%
50. R^1 = 4–$COCH_3$ I Yield = 77%
51. R^1 = 4–$CONH_2$ I Yield = 58%
52. R^1 = 4–$COOCH_3$ I Yield = 38%
53. R^1 = 4–NO_2 I Yield = 91%
54. R^1 = 4–CN I Yield = 74%
55. R^1 = 3,4–CH_3 I Yield = 74%
56. R^1 = 3,5–CH_3 I Yield = 73%
57. R^1 = 2,6–CH_3 I Yield = 47%
58. R^1 = 3,4,5–OCH_3 I Yield = 62%
59. R^1 = 3–OCH_2O–4 I Yield = 20%[a]
60. R^1 = 4-H I Yield = 63%

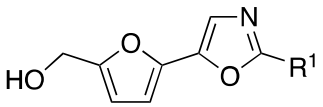

Scaffold B

61. R^1 = 4-pyridyl I Yield = 37%
62. R^1 = 3-pyridyl I Yield = 28%
63. R^1 = 1-naphthyl I Yield = 54%

Fig. 7. Structure and yield of compounds **32**–**63**, designed to combine features of both natural and synthetic products with known trypanocidal properties. [a]Reaction using an aryl bromide instead of an aryl iodide.

The natural alkaloids texamine (**27**), balsoxine (**29**), and uguenenazole (**21**) also were included in the study, and the effect of all compounds on *T. cruzi* viability was assessed. Seventeen of the thirty-one natural product analogs could reduce the parasite viability after 72 h of treatment. On the other hand, the alkaloids **27**, **29**, and **21** showed no effect on parasite

viability. This suggests that our strategy of molecular modification might have contributed to the biological activity, by either modulating PK or PD properties. The results are compiled in Table 3.

Table 3. Effect of the treatment (72 h) with compounds **32**–**63** in *T. cruzi* amastigotes (Tulahuen strain).

ID	Maximum activity (%)[a]	EC_{50} *T. cruzi* (µM)	CC_{50} THP-1 (µM)	SI
33	16.0 (±3.2)	–	–	–
34	28.5 (±0.7)	–	–	–
36	19.9 (±4.3)	–	–	–
37	23.6 (±10.7)	–	–	–
39	22.8 (±7.4)	–	–	–
40	14.6 (±3.9)	–	–	–
41	25.2 (±1.8)	–	–	–
42	18.8 (±14.0)	–	–	–
46	25.7 (±7.4)	–	–	–
47	74.3 (±7.1)	34.4 (±2.2)	282.2 (±46.6)	8.2
48	11.9 (±1.8)	–	–	–
49	54.0 (±6.9)	33.0 (±1.1)	157.6 (±7.4)	4.8
55	10.4 (±2.8)	–	–	–
59	50.1 (±3.1)	49.1 (±1.6)	550.9 (±16.8)	11.2
61	23.4 (±6.7)	–	–	–
60	31.6 (±1.2)	–	–	–
63	77.4 (±3.9)	24.2 (±1.4)	282.2 (±38.2)	11.7
21	NA	–	–	–
27	NA	–	–	–
29	NA	–	–	–
Bzn	99.5 (±1.8)	10.2 (±0.8)	–	>49

The results represent (average ± SD) of one experiment in triplicate. [a]Percentage of parasite death after the treatment with 50 µM of the compounds. NA = Not active [p >0.05 (ANOVA/Dunnet) in comparison with the negative control]. Bzn = Benznidazole. Compounds that led to more than 45% of parasite death were evaluated in different concentrations for EC_{50} and CC_{50} determination.

The results showed that most compounds are less active than the unsubstituted compound **60**, independently of the chemical nature of the substituent or the position in which they are linked to the aryl ring. 4-Position substitutions in the phenyl ring seem to the tolerated only for substituents with larger atomic radii and that are not strongly electron-withdrawing. Compounds **47**, **49**, **59**, and **63** are the most active in the entire series. The presence of bulky apolar substituents at the aryl ring of compounds **47**, **49**, and **63** contribute to increasing their

hydrophobicity, measured by *c*logP. It is known that high activity observed in compounds with high *c*logP could be justified by chemical features of some molecular targets: active sites are mostly located inside pockets, which makes the presence of apolar side chains of amino acids more likely. This favors hydrophobic interactions with ligands. Additionally, it also represents a challenge in drug design, as a hit compound should balance high potency with adequate PK properties.

Looking at compound **59**, although a 1,3-benzodioxole ring contributes to the bulkiness in the same region as in compounds **47**, **49**, and **63**, the presence of two heteroatoms in the ring counterbalances the lipophilicity of the substituent, and the compound shows lower *c*logP. This type of modification could be a strategy to obtain active compounds with friendlier physicochemical properties. The calculated solubility values (logP and logS) of the compounds are described in Supplementary Information, Table S1. Overall, these results introduce a new active scaffold and reinforce the importance of specific chemical features, such as the 1,3-benzodioxole ring, for the activity against *T. cruzi*.

2.3. The in vitro *potency of compound **5** increases when in combination with benznidazole*

The three most active compounds (**5**, **7**, and **8**) described in the previous sections were evaluated in combination (5 concentrations, 1:1 ratio, based on EC_{50} values) with benznidazol against *T. cruzi* (Tulahuen) in an additional *in vitro* assay. When two different compounds are evaluated in combination it is expected to observe a stronger biological response, called additive effect. Synergism and antagonism are situations in which the biological response is, respectively, superior, or inferior to that of additive effect [58]. Translating this to an *in vivo* context, the higher efficacy of a synergistic combination could impact the dose, treatment length, onset of side effects, and drug-related toxicity. The results of the combination studies are depicted in Table 4.

Table 4. Anti-trypanosomal activity (72 h) of compounds **5**, **7**, and **8** in combination with the drug benznidazole in *T. cruzi* amastigotes (Tulahuen strain)

Combination	Compound	Benznidazole	CI at the following inhibition[a]		
	EC_{50} (µM)	EC_{50} (µM)	50%	70%	90%
5 + Bzn (1:1)	0.0019	0.017	0.004	3.0	96162
7 + Bzn (1:1)	3.69	7.40	1.27	1.21	1.15
8 + Bzn (1:1)	3.33	4.36	0.91	0.86	0.80

[a]The CI value compares how much of a combination is needed to cause a biological effect (50, 70 and 90% inhibition), with the amount of the compounds needed when they are used alone. A combination is synergistic, additive or antagonistic if CI <1, =1, >1, respectively.

Compound **5** in combination with benznidazole has a strong synergistic effect (CI < 1) at the concentration that causes 50% of the parasite death. We observe a steady reduction in the EC_{50} of benznidazole and compound **5** in the combination when compared to individual EC_{50} values. The combination of compound **5** with benznidazole also dramatically reduced the cytotoxicity of compound **5** to THP 1 cells. In combinations containing concentrations up to 364 µM of compound **5**, no reduction in cell viability was observed.

Analyzing the data obtained at higher concentrations (70 and 90% inhibition), we observe that the combination of compound **5** with benznidazole is no longer synergistic but antagonistic instead. Similar dose-dependent results were observed in a study of drug combinations against *Aspergillus* species [59]. It is expected that concentration changes the nature of pharmacodynamic interactions, once side activities might become more prominent and counterbalance the effects seen in lower concentrations.

The combinations of compounds **7** and **8** with benznidazole are either weakly antagonistic or weakly synergistic, respectively. The change in pattern indicates that although structurally similar, the compounds have different biological behaviors. The presence of different halogens at the benzylic positions of compounds **5**, **7** and **8**, might hinder or contribute to putative intermolecular interactions, impacting the overall results observed in the combinations.

2.4. The treatment with the active compounds leads to mitochondrial membrane depolarization in T. cruzi epimastigotes

Kinetoplastida parasites have a single mitochondrion Different from mammalian cells, where hundreds of mitochondria are present, a malfunctioning in parasites might compromise life itself once the organelle is essential to synthesize energy as ATP. Multiple mitochondrial proteins have been described as targets of trypanocidal compounds. Besides, a change in the mitochondrial membrane potential (ΔΨm) after treatment is an indication that the organelle is being affected. Usually, the interplay among calcium, ATP, and reactive oxygen species (ROS), metabolism maintains ΔΨm and an unbalance in any of these could ultimately lead to parasite death. Structural changes that cause membrane permeability also affect ΔΨm [60–62].

We investigated the compounds active in the phenotypic assay regarding the effect they would cause in the ΔΨm in *T. cruzi* epimastigotes. After 24 h of treatment, the parasites were dyed with rhodamine-123 (Rh-123) and analyzed using flow cytometry. Rh-123 accumulates in the mitochondrial matrix and the measurement of its fluorescence can be used to determine ΔΨm [63]. The difference in median of Rh-123 fluorescence between untreated and treated parasites was used to calculate the ΔΨm index of variation, where negative values indicate membrane depolarization (Fig. 8a). Additionally, the parasites were dyed with propidium

iodide (PI) to evaluate whether the treatment with the compounds could also increase the permeability of their plasmatic membrane (Fig. 8b).

Among active lignan derivatives (Section 2.1), only compound **8** interfered with the ΔΨm of *T. cruzi* epimastigotes. On the other hand, all oxazole alkaloid derivatives (Section 2.2) affected the ΔΨm causing depolarization, notably compounds **47** and **49**. This indicates that although compounds in both series are structurally similar, they trigger different cellular events that ultimately lead to parasite death. In most cases the effect in ΔΨm was dose-dependent, reaching its maximum in the groups treated with eight times the EC_{50} of the compound (Fig. 8a). Compound **8** led to a strong depolarization of the mitochondrial membrane even in parasites treated with the lowest concentration (EC_{50}). The extent of the effect of compound **8** did not change significantly in parasites treated with up to eight times the initial concentration ($P > 0.05$).

The PI staining is additional evidence that the compounds do not necessarily act through the same pathway to cause parasite death. The treatment with compounds **8** (all concentrations), **47** (4 and 8 x EC_{50}), and **63** (8 x EC_{50}) led to the highest PI fluorescence, meaning that the plasmatic membrane integrity was affected by the treatment. Integrity loss of the plasmatic membrane is mostly associated with necrosis or late-stage apoptosis, which also could be triggered by oxidative stress. It is not clear whether the permeability of the mitochondrial membrane also has increased after treatment with these compounds, which could explain the observed depolarization. In all other treatment groups, the percentage of PI+ parasites was similar to that of the negative control (DMSO 1%). This could indicate that compounds **49** and **59** are slowly acting or that other cell death mechanisms might be activated in parasites after being treated with them (Fig. 8b).

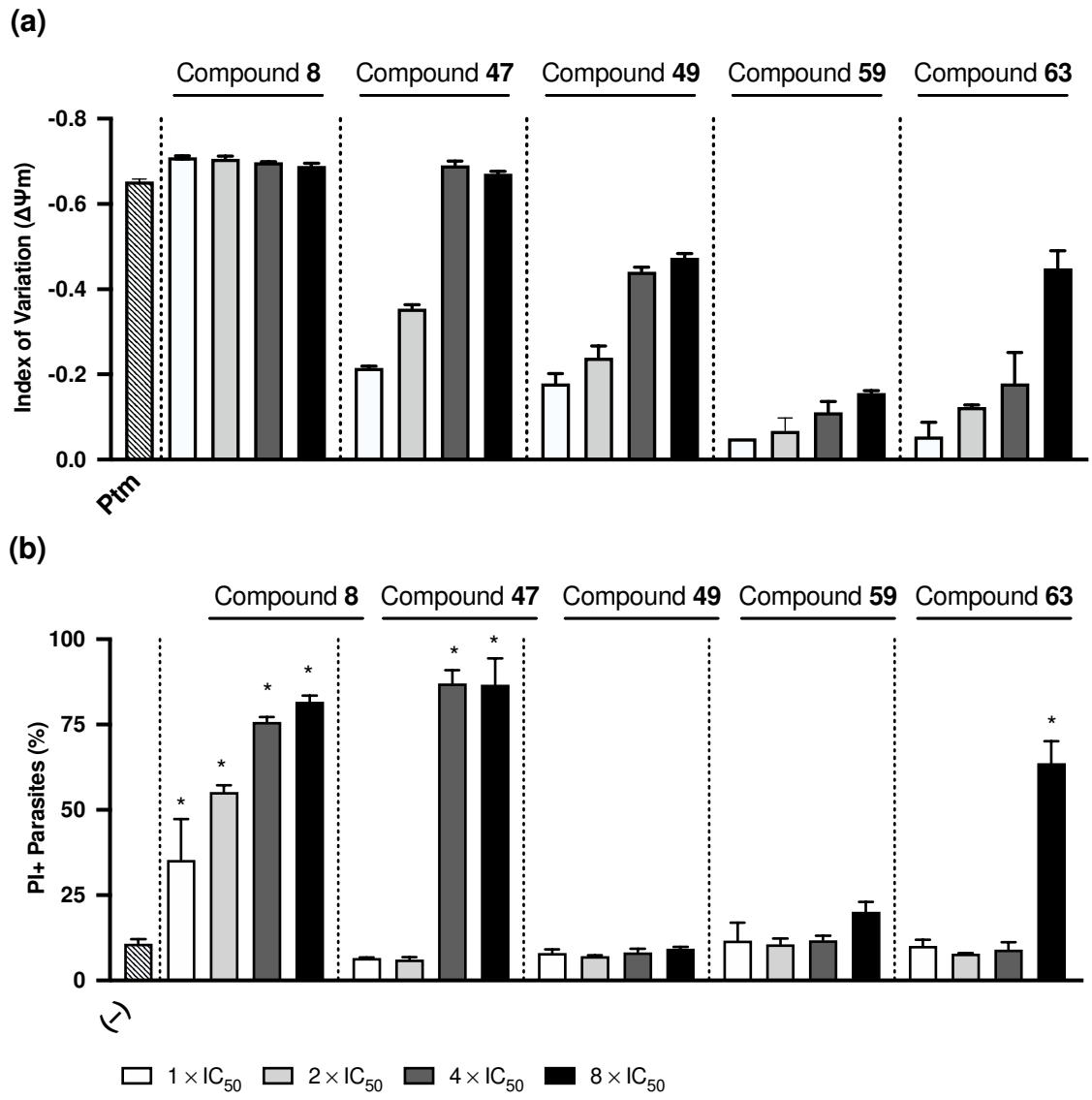

Fig 8. (a) ΔΨm index of variation calculated from Rh-123 signal intensity after 24 h of treatment. (b) Percentage of PI+ epimastigotes after 24 h of treatment. The bars represent average ± SD of triplicates. Ptm = Pentamidine 100 µM. (-) = DMSO 1%. Index of variation = (Rh-123 in treated parasites – Rh-123 in untreated parasites)/(Rh-123 in untreated parasites). *P <0.001 in comparison with the negative control (ANOVA/Dunnet).

2.5. Trypanothione reductase is not the molecular target though which the compounds exert their trypanocidal action

Trypanothione (*N*1,*N*8-Bis(glutathionyl)spermidine) is a glutathione analog present in Kinetoplastida parasites that acts in the cellular defense against oxidative stress. In the presence of ROS, trypanothione is oxidized to trypanothione disulfide. The enzyme trypanothione reductase (TryR, EC 1.8.1.12) is responsible for recycling trypanothione disulfide, maintaining the intracellular concentration of trypanothione in the levels needed for its biological role [64]. Although there are other enzymes involved in the metabolism of

trypanothione, TryR is the main target involved in the ROS metabolism explored for drug discovery in *T. cruzi*. Different classes of TryR inhibitors have already been identified and it is known that the inhibition of the enzyme also leads to reduced parasite viability in phenotypic models [65,66].

Considering that an increasing concentration of ROS is one of the causes of mitochondrial dysfunction, we investigated whether the inhibition of TyrR is involved in the mechanism of action of the compounds that were active in the phenotypic assay. However, the compounds did not inhibit the enzymatic activity in concentrations up to 100 µM. Additional assays are needed to determine which biological pathways are involved in the parasite death and mitochondrial effects caused by the treatment with the compounds presented herein.

2.6. The active compounds do not affect the membrane integrity of erythrocytes

We evaluated whether the active compounds **5**, **7**, **8**, **13**, **47**, **49**, **59**, and **63** could affect the plasma membrane integrity of human erythrocytes as a complementary step to assess their toxicity. After treating red-blood cells with 100 µM and 50 µM of the compounds no increase in the concentration of free hemoglobin was observed after 3 h for most compounds. The promising results in this endpoint indicate that the compounds are not haemotoxic, which is one of the requisites for in vivo testing.

Compound **47** in the concentration of 100 µM caused hemolysis in 37.7 (± 5.6)% of the cells. As compound **47** also led to a loss of membrane integrity in *T. cruzi* epimastigotes (Section 2.5), we might suggest that this effect is unspecific at higher concentrations. On the other hand, no hemolytic effect was observed in cells treated with 50 µM. This indicates a margin of at least 1.5 between the effective and the non-haemotoxic concentrations of compound **47**.

2.7. The active compounds share structural features with other known trypanocidal compounds

The seminal work of Lipinski brought to light that the number of polar heteroatoms and the molecular weight of chemical compounds affect their oral bioavailability [67]. Since then, multiple physicochemical descriptors have also been associated with properties required for small molecules having a good biological performance [68,69]. Therefore, an early assessment of chemical features such as the number of rotatable bonds, fraction of sp^3 hybridized carbons, aromatic ring count, and aqueous solubility (logS) can suggest whether a hit or lead compound needs further chemical optimization to maximize its probability of success within a drug development program. In addition, an integrative analysis of

physicochemical descriptors could bring information of similarities and differences between a group of compounds with known biological activity and hit compound candidates.

Hundreds of small molecules have been reported active against different life stages and strains of *T. cruzi*. For instance, an HTS campaign run by GlaxoSmithKline led to the identification of 222 new hit compounds (GSK Chagas box) [70]. These compounds were first selected using biological screening conditions similar to those employed herein. To visualize the chemical space occupied by these known trypanocidal molecules and analyze whether the compounds reported in our work fit similar space we used principal component analysis (PCA). Twenty physicochemical descriptors (Supplementary Information, Table S2) were obtained using Data Warrior (openmolecules.org/datawarrior/) and compiled into three principal components (PC), comprising 67% of the variance of the data [71].

In the PCA plot, we can observe that all analyzed compounds were highly distributed in the chemical space, demonstrating that different chemotypes might present activity against *T. cruzi* (Fig. 9). The main descriptors that contribute to PC1, 2, 3 are related to the presence of polar atoms in the molecules [such as HBA/HBD fraction (PC1), electronegative atoms, and H-acceptors (PC2)]. Additionally, we observe that molecular complexity descriptors [such as molecular complexity index (PC3), and the number of rings (PC4)] could be relevant to explain differences among molecules. Details are described in Supplementary Information, Table S2.

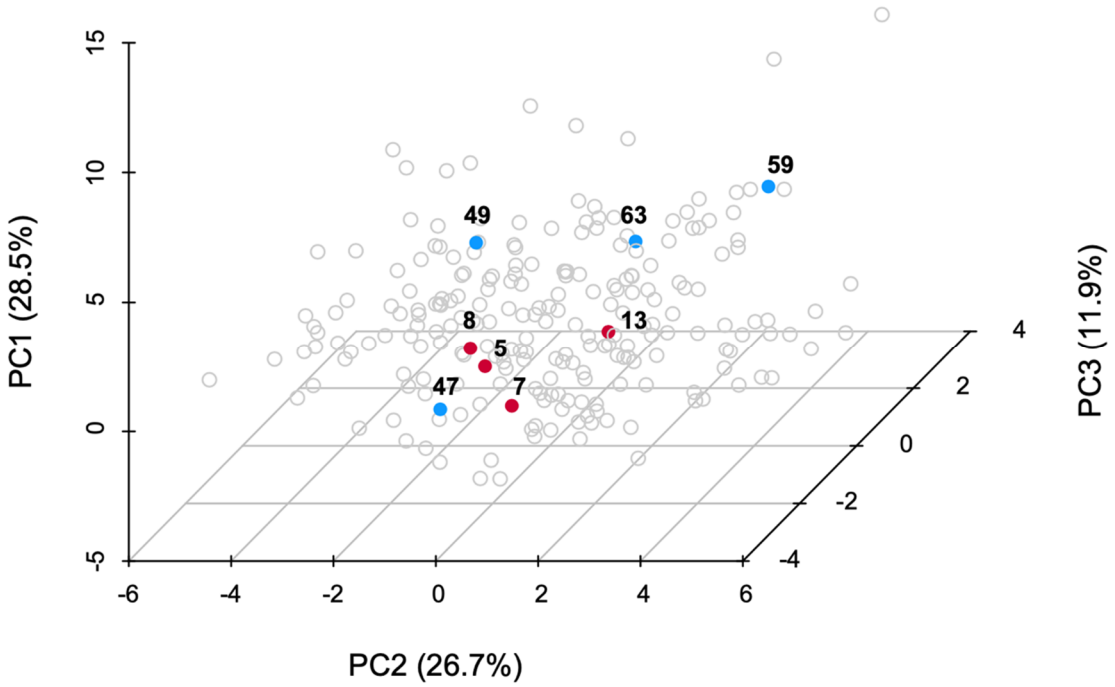

Fig 9. Principal component analysis (PCA) plot comparing physicochemical properties of 230 compounds active against *T. cruzi* in a phenotypic assay. GSK Chagas box compounds (n = 222) are represented as gray open circles and the active lignan- and alkaloid-based compounds presented in this work are represented as red and blue circles, respectively.

Overall, compounds **5**, **7**, **8**, **13**, **47**, **49**, **59**, and **63** share structural features with other active compounds and could give insights about structural elements required for biological activity or be further optimized to afford novel improved derivatives. Individual compounds reported in this work are not flagged in a Pan Assay Interference Compounds (PAINS) filter, supporting the validity of the biological results presented (as analyzed in SwissADME, swissadme.ch). Additionally, they fit common druglikeness "rules", suggesting they are predicted to have good pharmaceutical properties from an ADMET standpoint.

3. Conclusion

Natural products exhibit enormous potential as sources of inspiration for the design of biologically active molecules. Our results confirm that a nature-driven design of novel derivatives is an interesting strategy to obtain hit compounds with in vitro activity against *T. cruzi*. Multiple factors contribute to making drug discovery a challenging task, one of them being the understanding of complex chemical requirements for biological activity. Therefore, identification of such privileged scaffolds can foster the search for novel effective candidates that could advance drug development.

Seven compounds described in this study were highly active, with EC_{50} values in the low micromolar range. Compounds **7** and **8** are as potent as benznidazole in vitro. Moreover, compounds **5** and **8** act synergistically with benznidazole, meaning that reduced concentrations are necessary to achieve the same effects of individual treatments. The mechanisms leading to parasite death are not yet fully understood. However, there is an indication that compounds **8**, **47**, and **63** disrupt the integrity of the parasitic plasmatic membrane. Additional assays revealed that compounds **8**, **47**, **49**, **59**, and **63** also target parasitic mitochondria, affecting membrane potential. One of the causes of mitochondrial dysfunction is oxidative stress. Of note, compounds did not inhibit TryR, which is one of the main enzymes involved in ROS metabolism in *T. cruzi*. These compounds are nontoxic to uninfected cells (SI = 5–71) and erythrocytes (SI > 1.5), suggesting parasite specificity. The findings are an indication that compounds could show low toxicity in preclinical models of the disease.

As a next step, it is important to identify and understand which specific molecular mechanism is involved in the observed mitochondrial effect. Such knowledge could guide the design of more effective, target-directed derivatives using the herein described hit compounds as starting points.

Declaration of Competing Interest

The authors declare that they have no known competing financial interests or personal relationships that could have appeared to influence the work reported in this paper.

Acknowledgements

The authors are grateful for the access to the MS and NMR facilities at the Université Lyon 1 (CCRMN and CCSM) and the Universidade Federal de Santa Catarina (UFSC, CIF). We are also grateful for the access to the LAMEB facilities at UFSC (CCB).

Funding

This work was supported by the Brazilian funding agencies CNPq [grant number 407626/2016-6] and CAPES [scholarships number 88887.364922/2019-00 (DS) and 88882.438170/2019-01 (PrInt)].

4. Materials and Methods

4.1. Chemistry

All reagents and solvents were purchased from commercial sources and used in the experiments without further purifications, unless stated otherwise. ^{1}H and ^{13}C NMR data were acquired on a Bruker Fourier 300 (^{1}H 300 MHz, ^{13}C 75 MHz) or Bruker 400 (^{1}H 400 MHz, ^{13}C 100 MHz) at 298 K using $CDCl_3$, DMSO-d_6 or CD_3OD as solvents. The NMR spectra were calibrated using an internal standard (TMS δ 0.00) or the residual non-deuterated solvent peak (FULMER et al., 2010). The chemical shifts (δ) are reported in ppm and the coupling constants (*J*) in hertz. The following abbreviations or the combination of them are used for the multiplicities: s = singlet, d = doublet, t = triplet, q = quartet, dd = doublet of doublets, m = multiplet. High-resolution mass spectra (HRMS) were recorded on a Finnigan Mat 95xL or on Waters XEVO G2-S QToF mass spectrometer using electrospray (ESI). Analytical thin-layer chromatography was run on silica gel Merck 60 D254 (0.25 mm) plates. Column chromatography was performed on silica gel HF_{254} (40–63 μm) using different combinations of hexane, pentane, ethyl acetate, acetone, or dichloromethane as eluent. Melting points were measured using a Büchi apparatus B-540 or a Microquímica apparatus MQAPF-301 and are reported uncorrected.

*4.1.1. Synthesis of 3-(3,4-benzodioxole)-5-(4-hydroxymethylphenyl)isoxazole (**4**)*

Compound **4** was synthesized using a previously published method [40]. ^{1}H NMR (400 MHz, $CDCl_3$): δ 7.83 (d, *J* = 8.5, 2H), 7.50 (d, *J* = 8.5, 2H), 7.39 (d, *J* = 1.8 Hz, 1H), 7.34 (dd, *J* = 1.8, 8.1, 1H), 6.91 (d, *J* = 8.1, 1H), 6.75 (s, 1H), 6.04 (s, 2H), 4.78 (s, 2H). 13C NMR (100

MHz, CD_3OD): δ 171.5, 164.1, 150.8, 149.7, 145.4, 128.4, 127.5, 126.8, 124.0, 122.4, 109.6, 107.6, 102.9, 98.6, 64.6. HRMS (ESI-TOF) m/z: $[M+H]^+$ Calcd for $C_{17}H_{14}NO_4$ 296.0923; Found 296.0891. MP °C: 180.1–181.4.

*4.1.2. Synthesis of 3-(3,4-benzodioxole)-5-(4-chloromethylphenyl)isoxazole (**5**)*

Compound **4** (0.85 mmol, 25 mg, 1 eq) was solubilized in anhydrous CH_2Cl_2 (1 mL) and maintained under N_2. Thionyl chloride (3 eq) was added dropwise, and the solution was stirred at room temperature until the complete conversion of the starting material (approximately 1 h). At the end, the reactional mixture was placed in an ice bath, diluted with 15 mL of CH_2Cl_2 and washed with brine (3 x 10 mL). The organic layers were dried over anhydrous Na_2SO_4, filtered, and the solvent was removed under vacuum. The product was obtained as a yellow solid (25 mg, 94% yield) after purification (SiO_2, hexane:ethyl acetate 7:3). ^1H NMR (300 MHz, $CDCl_3$): δ 7.82 (d, *J* = 8.4, 2H), 7.51 (d, *J* = 8.4, 2H), 7.38 (d, *J* = 1.7, 1H), 7.34 (dd, *J* = 8.0, 1.7, 1H), 6.90 (d, *J* = 8.0, 1H), 6.77 (s, 1H), 6.05 (s, 2H), 4.64 (s, 2H). ^{13}C NMR (75 MHz, $CDCl_3$): δ 169.6, 163.2, 149.2, 148.2, 139.4, 129.2, 127.4, 122.9, 121.2, 106.6, 101.5, 97.7, 46.6. HRMS- ESI: m/z $[M+H]^+$ Cald for $C_{17}H_{13}ClNO_3$ 314.0584; Found 314.0576. MP °C: 162.1–163.2.

*4.1.3. Synthesis of 3-(3,4-benzodioxole)-5-(4-bromomethylphenyl)isoxazole (**6**)*

Compound **6** was synthesized from product **4** using the same procedure used for the synthesis of compound **5**. However, thionyl bromide (3 eq) was used instead of thionyl chloride (3 eq). The product was obtained as a yellow solid (25 mg, 82% yield) after purification (SiO_2, hexane: ethyl acetate 7:3). ^1H NMR (300 MHz, $CDCl_3$): δ 7.82 (d, *J* = 8.4, 2H), 7.52 (d, *J* = 8.4, 2H), 7.39 (d, *J* = 1.7, 1H), 7.35 (dd, *J*= 8.0, 1.7, 1H), 6.92 (d, *J*= 8.0, 1H), 6.77 (s, 1H), 6.06 (s, 2H), 4.54 (s, 2H). ^{13}C NMR (75 MHz, $CDCl_3$): δ 169.6, 162.6, 149.2, 148.3, 139.8, 129.7, 127.4, 126.2, 122.9, 121.2, 108.7, 101.5, 97.7, 32.6. HRMS-ESI: m/z $[M+H]^+$ Calcd for $C_{17}H_{13}BrNO_3$ 358.0079; Found 358.0074. MP °C: 173.7–175.0.

*4.1.4. Synthesis of 3-(3,4-benzodioxole)-5-(4-fluoromethylphenyl)isoxazole (**7**)*

Compound 4 (0.85 mmol, 25 mg, 1 eq) was solubilized in anhydrous CH_2Cl_2 (1 mL), placed in an ice bath, and maintained under N_2. Deoxo-Fluor® (1.05 eq) was added to the solution dropwise. The ice bath was removed, and the reactional mixture was stirred for 20 h at room temperature. At the end, a $NaHCO_3$ 5% solution (10 mL) was added, and the reactional mixture was extracted with CH_2Cl_2 (3 x 10 mL). The organic layers were dried over anhydrous Na_2SO_4, filtered, and the solvent was removed under vacuum. The product was obtained as a white solid (3 mg, 4% yield) after purification (SiO_2, hexane:ethyl acetate 7:3). ^1H NMR (300 MHz, $CDCl_3$): δ 7.87 (d, *J* = 8.1, 2H), 7.50 (d, *J* = 8.1, 2H), 7.38 (d, *J* = 1.5, 1H), 7.34 (dd, *J* =

1.5, 8.0, 1H), 6.91 (d, *J* = 8.0, 1H), 6.78 (s, 1H), 6.05 (s, 2H), 5.45 (d, *J* = 47.5, 2H, CH_2F). HRMS-ESI: m/z $[M+H]^+$ Calcd for $C_{17}H_{13}FNO_3$ 297.0801; Found 297.0869.

*4.1.5. Synthesis of 3-(3,4-benzodioxole)-5-(4-iodomethylphenyl)isoxazole (**8**)*

Compound **5** (0.08 mmol, 25 mg, 1 eq) and KI (1.2 eq) were solubilized in acetone (1 mL). The reaction was stirred for 20 h at room temperature. At the end the reaction diluted with 15 mL of CH_2Cl_2 and washed with brine (3 x 10 mL). The organic layers were dried over anhydrous Na_2SO_4, filtered, and the solvent was removed under vacuum. The product was obtained as a white solid (13 mg, 40% yield) after purification (SiO_2, hexane:ethyl acetate 7:3). ^1H NMR (300 MHz, $CDCl_3$): δ = 7.76 (d, *J* = 8.3, 2H), 7.49 (d, *J* = 8.3, 2H), 7.38 (d, *J* = 1.7, 1H), 7.34 (dd, *J* = 8.0, 1.7, 1H), 6.91 (d, *J* = 8.0, 1H), 6.75 (s, 1H), 6.04 (s, 2H), 4.50 (s, 2H). ^{13}C NMR (75 MHz, $CDCl_3$): δ 169.6, 162.7, 149.2, 148.2, 141.5, 129.4, 126.8, 126.3, 122.9, 121.2, 108.6, 107.0, 101.5, 97.6, 4.5. HRMS-ESI: m/z $[M+H]^+$ Calcd for $C_{17}H_{13}INO_3$ 405.9940; Found 405.9931. MP °C: 165.8–167.0.

4.1.6. Synthesis of 3,4-methylenedioxybenzyl-4-(chloromethyl)benzoate (**10**)

4-chloromethylbenzoic acid (0.14 mmol, 25 mg, 1 eq) was solubilized in anhydrous CH_2Cl_2 (3 mL) and maintained under N_2. Thionyl chloride (3 eq) was added dropwise, and the solution was stirred at reflux temperature until the complete conversion of the starting material (approximately 2 h). The solvent and the excess of thionyl chloride were removed under vacuum and the crude reactional mixture was again solubilized in anhydrous CH_2Cl_2 (3 mL) and maintained under N_2. 3,4-methylenedioxybenzyl alcohol in anhydrous CH_2Cl_2 (2 mL) was added dropwise and the reactional mixture was stirred at room temperature for 1 h. At the end, the reactional mixture was placed in an ice bath, diluted with 15 mL of CH_2Cl_2 and washed with aqueous $NaHCO_3$ 5% and brine (3 x 10 mL). The organic layers were dried over anhydrous Na_2SO_4, filtered, and the solvent was removed under vacuum. The product was obtained as a white solid (40 mg, 94% yield) after purification (SiO_2, hexane:ethyl acetate 8:2). ^1H NMR (300 MHz, $CDCl_3$): δ 8.06 (d, *J* = 8.1, 2H), 7.47 (d, *J* = 8.1, 2H), 6.99 – 6.90 (m, 2H), 6.82 (d, *J* = 7.6, 1H), 5.99 (s, 2H), 5.27 (s, 2H), 4.62 (s, 2H). ^{13}C NMR (75 MHz, $CDCl_3$): δ 165.9, 147.8, 142.3, 130.13, 130.08, 129.6, 128.5, 122.3, 109.0, 108.3, 101.2, 66.8, 45.4. HRMS-ESI: m/z $[M+H]^+$ Calcd para $C_{16}H_{13}ClNaO_4$ 327.0400; Found 327.0404. MP °C: 71.2–72.1.

*4.1.7. Synthesis of N-(3,4-methyelendioxybenzyl)-4-(chloromethyl)benzamide (**11**)*

4-chloromethylbenzoic acid (0.14 mmol, 25 mg, 1 eq) was solubilized in anhydrous THF (1 mL) and *N,N*-carbonyldiimidazole (1.1 eq) was slowly added to the solution. The reactional mixture was stirred at room temperature for 30 minutes and then piperonylamine (1.1 eq) was

added and the reaction was maintained under stirring for 20 h. At the end, brine (15 mL) was added, and the reactional mixture was extracted with CH_2Cl_2 (3 x 10 mL). The organic layers were dried over anhydrous Na_2SO_4, filtered, and the solvent was removed under vacuum. The product was obtained as a white solid (12 mg, 27% yield) after purification (SiO_2, hexane:ethyl acetate 6:4).

^{1}H NMR (300 MHz, $CDCl_3$): δ 7.77 (d, *J* = 8.4, 2H), 7.44 (d, *J* = 8.4, 2H), 6.85–6.78 (m, 2H), 6.76 (d, *J* = 7.9, 1H), 6.43 (t, *J* = 5.7, 1H), 5.95 (s, 2H), 4.60 (s, 2H), 4.54 (d, *J* = 5.7, 2H). ^{13}C NMR (75 MHz, $CDCl^3$): δ 166.7, 148.0, 147.1, 140.9, 134.2, 133.9, 128.7, 127.4, 121.3, 108.5, 108.4, 101.1, 45.8, 44.0. HRMS-ESI: m/z $[M+H]^+$ Calcd para $C_{16}H_{15}ClNO_3$ 304.0740; Found 304.0744. MP °C: 123.6–124.7.

*4.1.8. Synthesis of N'-((4-(chloromethyl)benzoyl)oxy)3,4-methylenedioxyphen-1-yl-5-carboxyimidamide (**12**)*

4-chloromethylbenzoic acid (0.28 mmol, 47 mg, 1 eq) and *N,N*-carbonyldiimidazole (0.56 mmol, 94 mg, 2 eq) in anhydous DMF (1 mL) were stirred at room temperature for 30 minutes. 3,4-methylenedioxyphenylamidoxime (0.28 mmol, 50 mg, 1 eq) was added and the reaction maintained under stirring overnight. At the end, brine (25 mL) was added, and the reactional mixture was extracted with CH_2Cl_2:MeOH (1:1 v/v, 4 x 10 mL). The organic layers were dried over anhydrous Na_2SO_4, filtered, and the solvent was removed under vacuum. The product was obtained as a white solid (69 mg, 74% yield) after purification (SiO_2, hexane:ethyl acetate 4:6). ^{1}H NMR (300 MHz, $CDCl_3$): δ 8.16 (d, *J* = 8.3, 2H), 7.60 (d, *J* = 8.3, 2H), 7.40 (dd, *J* = 1.8, 8.2, 1H), 7.34 (d, *J* = 1.4, 1H), 6.92 (d, *J* = 8.2, 1H), 6.08 (s, 2H), 4.81 (s, 2H). ^{13}C NMR (75 MHz, $CDCl_3$): δ 163.8, 157.7, 150.6, 148.7, 143.6, 130.9, 130.8, 129.6, 126.6, 122.0, 108.8, 107.8, 102.6, 46.0. HRMS-ESI: m/z $[M+Na]^+$ Calcd for $C_{16}H_{13}ClN_2O_4Na$ 355.0462, found 355.0481. MP °C: 150.4–151.8.

*4.1.9. Synthesis of 3-(3,4-methylenedioxyphen-1-yl)-5-(4-chloromethylphen-1-yl)1,2,4-oxadiazole (**13**)*

Compound **12** (0.075 mmol, 25 mg, 1 eq) was heated in anhydrous DMF (1 mL, 80 ºC) until full conversion (approximately 4 h). At the end, brine (25 mL) was added, and the reactional mixture was extracted with CH_2Cl_2:MeOH (1:1 v/v, 4 x 10 mL). The organic layers were dried over anhydrous Na_2SO_4, filtered, and the solvent was removed under vacuum. The product was obtained as a white solid (21 mg, 89% yield) after purification (SiO_2, hexane:ethyl acetate 4:6). ^{1}H NMR (300 MHz, acetona-d_6): δ 8.23 (d, *J* = 8.5, 2H), 7.75 (d, *J* = 8.5, 2H), 7.74 (dd, *J* = 1.7, 8.1; 1H), 7,55 (d, *J* = 1.7, 1H), 7.05 (d, *J* = 8.1, 1H), 6.15 (s, 2H), 4.86 (s, 2H). ^{13}C NMR (75 MHz, acetona-d_6): δ 176.0, 169.4, 151.4, 149.4, 144.0, 130.6, 129.3, 124.9, 123.2, 121.6,

109.6, 107.8, 103.0, 46.0. HRMS-ESI: m/z $[M+H]^+$ Calcd for $C_{16}H_{12}ClN_2O_3$ 315.0536, found 315.0526. MP °C: 152.0–152.7.

*4.1.10. Synthesis of 1-(3,4-methylenedioxybenz-1-yl)-N-(4-chloromethyl)benzylamine (**16**)*

4-chloromethylbenzaldehyde (0.16 mmol, 25 mg, 1 eq) and piperonylamine (1 eq) were solubilized in anhydrous CH_2Cl_2 (1 mL). The reaction was maintained under stirring until full conversion of the starting materials to the imide intermediate. Then, $NaBH_4$ (1 eq) and a few drops of methanol were added to the reaction. At the end, the reactional mixture was diluted in methanol (25 mL), filtered in a Celite® pad and concentrated under vacuum. The product was obtained as a white solid (16 mg, 35% yield) after purification (Al_2O_3, hexane:ethyl acetate 1:1). ^{1}H NMR (300 MHz, $CDCl_3$): δ 7.30–7.43 (m, 4H), 6.88 (s, 1H), 6.74–6.82 (m, 2H), 5.94 (s, 2H), 4.58 (s, 2H), 3.78 (s, 2H), 3.70 (s, 2H). ^{13}C NMR (75 MHz, $CDCl_3$): δ 147.7, 146.6, 140.6, 136.2, 13.0, 128.7, 128.5, 121.3, 108.7, 108.1, 100.9, 52.9, 52.5, 46.2. HRMS-ESI: m/z $[M+H]^+$ Calcd for $C_{16}H_{17}ClNO_2$ 290.0948; found 290.0952. MP °C: Liquid at room temperature.

*4.1.11. Synthesis of (E)-1-(3,4-methylenedioxyphenyl)-3-(4-(chloromethyl)phenyl)prop-2-en-1-one (**17**)*

3,4-methylenedioxyacetophenone (0.15 mmol, 25 mg, 1 eq) and 4-chloromethylbenzaldehyde (1 eq) were added to a methanolic solution of NaOH 10% (m/v). The reaction was maintained under stirring until full conversion of the starting materials (approximately 4 hours). At the end, $HCl_{(aq)}$ 0.1 mol L^{-1} was added for neutralizing the reactional mixture and EtOAc (3x 10 mL) was used for extracting the product. The organic layers were dried over anhydrous Na_2SO_4, filtered, and the solvent was removed under vacuum. The product was obtained as a yellow solid (35 mg, 75% yield) after purification (SiO_2, hexane:ethyl acetate 6:4). ^{1}H NMR (300 MHz, $CDCl_3$): δ 7.71 (d, *J* = 15.7, 1H), 7.61–7.54 (m, 3H), 7.47 (d, *J* = 1.7, 1H), 7.43 (d, *J* = 15.7, 1H), 7.37 (d, *J* = 8.0, 2H), 6.83 (d, *J* = 7.8, 1H), 6.00 (s, 2H), 4.54 (s, 2H). ^{13}C NMR (75 MHz, $CDCl_3$): δ 188.1, 151.8, 148.4, 143.4, 139.6, 135.1, 132.8, 129.2, 128.7, 124.8, 122.2, 108.4, 108.0, 101.9, 45.7. HRMS-ESI: m/z $[M+H]^+$ Calcd for $C_{17}H_{14}ClO_3$ 301.0631; found 301.0624. MP °C: 143.0–144.7.

*4.1.12. Synthesis of 3-(3,4-methylenedioxyphen-1-yl)-5-(4-hydroxymethylphen-1-yl)isoxazoline (**19**)*

3,4-methylenedioxybenzaldoxime (0.12 mmol, 20 mg, 1 eq) and *N*-chloro succinimide (1.2 eq) were dissolved in CH_2C_{l2} (1 mL) and maintained under stirring until full conversion of the starting material. Then, triethylamine (1.2 eq) and 4-vinylbenziylic alcohol (1.2 eq) were added and the reactional mixture was kept stirring for 2 more hours. At the end, brine (15 mL) was

added, and the reaction was extracted with EtOAc (3 x 10 mL). The organic layers were dried over anhydrous Na_2SO_4, filtered, and the solvent was removed under vacuum. The product was obtained as a white solid (25 mg, 27% yield) after purification (SiO_2, hexane:ethyl acetate 6:4). ^{1}H NMR (300 MHz, $CDCl_3$): δ 7.40 (s, 4H), 7.34 (d, *J* = 1.7 Hz, 1H), 7.06 (dd, *J* = 1.7, 8.2 Hz, 1H), 6.83 (d, *J* = 8.2, 1H), 6.03 (s, 2H), 5.72 (dd, *J* = 8.2, 11.2; 1H), 4.72 (s, 2H), 3.74 (dd, *J* = 11.2; 16.5, 1H), 3.29 (dd, *J* = 8.2, 16.5, 1H). ^{13}C NMR (75 MHz, $CDCl_3$): δ 155.7, 149.4, 148.1, 140.9, 140.3, 127.4, 126.1, 123.6, 121.6, 108.2, 106.6, 101.5, 82.3, 65.0, 43.4. HRMS-ESI: m/z $[M+H]^+$ Calcd for $C_{17}H_{16}NO_4$ 298.1079, found 298.1065. MP °C: 123.0–124.1.

*4.1.13. Synthesis of 3-(3,4-methylenedioxyphen-1-yl)-5-(4-chloromethylphen-1-yl)isoxazoline (**20**)*

Compound **20** was synthesized from compound **19** (0.067 mmol, 20 mg, 1 eq) using the same procedure described for the synthesis of compound **5**. The product was obtained as a yellow solid (15 mg, 71% yield) after purification (SiO_2, hexane:ethyl acetate 8:2). ^{1}H NMR (300 MHz, $CDCl_3$): δ 7.39 (s, 4H), 7.32 (d, *J* = 1.6, 1H), 7.03 (dd, *J* = 1.6, 8.0, 1H), 6.82 (d, *J* = 8.0, 1H), 6.02 (s, 2H), 5.72 (dd, *J* = 8.0, 11.0, 1H), 4.59 (s, 2H). 3.74 (dd, *J* = 11.0, 16.5, 1H), 3.27 (dd, *J* = 8.0, 16.5, 1H). ^{13}C NMR (75 MHz, $CDCl_3$): δ 155.8, 149.5, 148.2, 141.4, 137.6, 129.1, 126.4, 123.5, 121.7, 108.3, 106.6, 101.6, 82.1, 46.0, 43.6. HRMS-ESI: m/z $[M+H]^+$ Calcd for $C_{17}H_{15}ClNO_3$ 316.0740, found 316.0736. MP °C: 117.2–119.0.

*4.1.14. Synthesis of 1-(3,4-methylenedioxyphen-1-yl)-4-(4-hydroxymethylphen-1-yl)triazole (**22**)*

Piperonylamine (0.36 mmol, 50 mg, 1 eq) was added to HCl 6N (2 mL) and maintained in an ice bath. Sodium nitrite (1.5 eq) was slowly added to the solution and the reactional mixture was stirred for 30 minutes. Then, sodium azide (4 eq) dissolved in 0.5 mL of water was added and the reaction was maintained under stirring at room temperature for 2 hours. At the end, brine (25 mL) was added, and the reactional mixture was extracted with EtOAc (3 x 10 mL). The organic layers were dried over anhydrous Na_2SO_4, filtered, and the solvent was removed under vacuum. The crude reactional mixture was dissolved in DMF (1 mL) and transferred to a microwave tube. 4-ethynylbenzyl alcohol (1.05 eq), sodium ascorbate (10 mol%), copper(II) sulfate (2 mol%) were added to the tube. The reactional mixture was irradiated for 10 minutes (70 °C) and we proceeded with the work-up in the same way as in the previous step. The product was obtained as a dark yellow solid (28 mg, 26% yield) after purification (SiO_2, hexane:ethyl acetate 6:4). ^{1}H NMR (300 MHz, acetone-d_6): δ 8.86 (s, 1H), 7.94 (d, *J* = 8.0, 2H), 7.49–7.45 (m, 3H), 7.44 (dd, *J* = 8.3, 2.2, 1H), 7.06 (d, *J* = 8.3, 1H), 6.17 (s, 2H), 4.69 (d, *J* = 5.4, 2H), 4.34 (t, *J* = 5.4, 1H). ^{13}C NMR (75 MHz, acetone-d_6): δ = 149.5, 148.7, 148.4,

143.4, 130.2, 127.7, 126.1, 119.5, 114.6, 109.2, 103.1, 102.7, 64.3. HRMS-ESI: m/z $[M+H]^+$ Calcd for $C_{16}H_{14}N_3O_3$ 296.1035, found 296.1033. MP °C: 177.3-178.9.

*4.1.15. Synthesis of 1-(3,4-methylenedioxyphen-1-yl)-4-(4-chloromethylphen-1-yl)triazole (**23**)*

Compound **23** was synthesized from compound **22** (0.04 mmol, 12 mg, 1 eq) using the same procedure described for the synthesis of compound **5**. The product was obtained as a yellow solid (10 mg, 78% yield) after purification (SiO_2, hexane:ethyl acetate 8:2). ^1H NMR (300 MHz, $CDCl_3$): δ 8.10 (s, 1H), 7.90 (d, *J* = 8.2, 2H), 7.49 (d, *J* = 8.2, 2H), 7.31 (d, *J* = 1.7, 1H), 7.20 (d, *J* = 1.7, 8.3, 1H), 6.93 (d, *J* = 8.3, 1H), 6.10 (s, 2H), 4.64 (s, 2H). ^{13}C NMR (75 MHz, $CDCl_3$): δ 148.7, 148.2, 147.4, 137.7, 131.4, 129.7, 126.2, 118.3, 114.3, 108.6, 102.8, 102.2, 46.0. HRMS-ESI: m/z $[M+H]^+$ Calcd for $C_{16}H_{13}ClN_3O_2$ 314.0696, found 314.0689. MP °C: 197.4–199.0.

*4.1.16. Procedure for the synthesis of compounds **32–41**, **44**, **46–52**, and **55–63**.*

2-oxazolyl-5-hydroxymethyl-furan (0.30 mmol, 50 mg, 1 eq), an aryl iodide (0.36 mmol, 1.2 eq), $Pd(OAc)_2$ (0.0030 mmol, 7 mg, 10 mol%), anhydrous K_2CO_3 (0.60 mmol, 82 mg, 2 eq) and CuI 99.999% (0.30 mmol, 57 mg, 1 eq) were added to a oven-dried reaction tube. The reactional mixture was sealed with a septum and evacuated in the Schlenk line (three vacuum-nitrogen cycles). Anhydrous DMF (1 mL) was added and the reaction was maintained at 100 °C for 24 hours. At the end, the reaction was diluted in methanol, filtered through a Celite® pad and concentered under vacuum. The purification of the final compounds was done by column chromatography (SiO_2, pentane:ethyl acetate). The spectral details of the compounds are available in a previous publication of our research group [57].

*4.1.17. Procedure for the synthesis of compounds **25**, **42**, **43**, **45**, **53** and **54**.*

2-oxazolyl-5-hydroxymethyl-furan (0.30 mmol, 50 mg, 1 eq) or 3,4-methylenedioxyphen-1-yloxazole (0.26 mmol, 50 mg, 1 eq), aryl-iodide [*p*-hydroxymethyliodobenzene, *p*-cyano-iodobenzene, *p*-nitro-iodobenzene, *o*-chloro-iodobenzene, *m*-fluor-iodobenzene, or *m*-chloro-iodobenzene (0.36 mmol, 1.2 eq), triphenylphosphine (0.0060 mmol, 15 mg, 20 mol%)], anhydrous K_2CO_3 (0.60 mmol, 82 mg, 2 eq) and CuI 99.999% (0.30 mmol, 57 mg, 1 eq) were added to a oven-dried reaction tube. The reactional mixture was sealed with a septum and evacuated in the Schlenk line (three vacuum-nitrogen cycles). Anhydrous DMF (1 mL) was added and the reaction was maintained at 100 °C for 24 hours. At the end, the reaction was diluted in methanol, filtered through a Celite® pad and concentered under vacuum. The purification of the final compounds was done by column chromatography (SiO_2, pentane:ethyl

acetate). The spectral details of the compounds are available in a previous publication of our research group [57].

*4.1.18. Synthesis of 2-(4-hydroxymethylphen-1-yl)-5-(3,4-methylenedioxyphen-1-yl)oxazole (**25**)*

Compound **25** was synthesized as described in item 4.1.17. The product was obtained as a yellow solid (25 mg, 33% yield) after purification (SiO_2, hexane:ethyl acetate 1:1). ^{1}H NMR (300 MHz, acetona-d_6): δ 8.09 (d, *J* = 8.4, 2H), 7.56 (s, 1H), 7.53 (d, *J* = 8.4, 2H), 7.38 (dd, *J* = 1.7, 8.3; 1H), 7.36 (d, *J* = 1.7, 1H), 6.97 (d, *J* = 8.3, 1H), 6.08 (s, 2H), 4.72 (d, *J* = 5.8, 2H), 4.44 (t, *J* = 5.8; 1H). ^{13}C NMR (75 MHz, acetona-d_6): δ 160.4, 151.8, 149.2, 148.8, 145.9, 127.6, 126.9, 126.7, 123.5, 123.0, 119.0, 109.6, 105.3, 102.4, 64.1. HRMS-ESI: m/z $[M+H]^+$ Calcd para $C_{17}H_{14}NO_4$ 296.0923, found 296.0933. MP °C: 173.0–174.8.

*4.1.19. Synthesis of 2-(4-chloromethylphen-1-yl)-5-(3,4-methylenedioxyphen-1-yl)oxazole (**26**)*

Compound **26** was synthesized from compound **25** (0.004 mmol, 10 mg, 1 eq) using the same procedure described for the synthesis of compound **5**. The product was obtained as a yellow solid (10 mg, 94% yield) after purification (SiO_2, hexane:ethyl acetate 8:2). ^{1}H NMR (300 MHz, $CDCl_3$): δ 8.08 (d, *J* = 8.4, 2H), 7.50 (d, *J* = 8.4, 2H), 7.32 (s, 1H), 7.24 (dd, *J* = 8.2, 1.7, 1H), 7.18 (d, *J* = 1.7, 1H), 6.89 (d, J = 8.2, 1H), 6.03 (s, 2H), 4.64 (s, 2H). ^{13}C NMR (75 MHz, $CDCl_3$): δ 160.1, 151.3, 148.2, 148.0, 139.4, 129.1, 127.4, 126.5, 122.4, 122.1, 118.4, 108.9, 104.8, 101.4, 45.7. HRMS-ESI: m/z $[M+H]^+$ Calcd for $C_{17}H_{13}ClNO_3$ 314.0584, found 314.0586. MP °C: 134.6–135.9.

4.2. Biology

4.2.1. Parasites and cells

T. cruzi trypomastigotes (Tulahuen strain) expressing β-galactosidase were cultivated in a mice fibroblast cell line (L929, ATCC CCL-1) in 75 cm^2 cell culture bottles. RPMI-1640 without phenol red (10 mL), supplemented with 10% FBS, 10 U/mL of penicillin, and 10 µg/mL of streptomycin was used as culture medium.

THP-1 cells (ATCC TIB 202TM) were cultivated in 75 cm^2 cell culture bottles. RPMI-1640 without phenol red (12 mL), supplemented with 10% FBS, 2 mM of glutamax, 1 mM of sodium pyruvate, 10 U/mL of penicillin, and 10 µg/mL of streptomycin was used as culture medium

All cell cultures were maintained at 37°C, 5% de CO_2, and the cells were passaged every 3–4 days.

4.2.2. Stock and test solutions preparation

The chemical compounds were weighted in an analytical balance and solubilized to 50 mM using DMSO prior to the assays. From this stock solution, the test solutions were prepared using RPMI-1640 as diluent. The maximum DMSO concentration in the final cell culture was 1%. The stock solutions were not stored for more than 24 h.

4.2.3. Biological activity against intracellular amastigotes of T. cruzi.

THP-1 cells were cultivated in 96 well plates (4.0×10^4 cells/well) in 10% SBF supplemented RPMI-1640. The cells were treated with 100 ng/ml of phorbol 12-myristate 13-acetate (PMA) for 72 h (37 °C, 5% CO_2) to allow cell differentiation into non-dividing macrophages. Then, THP-1 cells were incubated with cell-culture-derived *T. cruzi* trypomastigotes in a parasite/cell ratio of 2:1 overnight (37 °C, 5% CO_2). Next, non-adherent parasites were removed by washing with PBS and infected cells incubated with 180.0 µL of full supplemented RPMI-1640 medium for another 24 h (37 °C, 5% CO_2) to allow the parasite differentiation into intracellular amastigotes. Inittially, the compounds were screened at a single concentration (50 µM) in a 72 h treatment. At the end of the treatment time, cells were washed with PBS and incubated for 16 h (37 °C, 5% CO_2) with 250.0 µL of chlorophenolred-ß-d-galactopyranoside (Sigma–Aldrich Co., St. Louis, MO, USA) at 100 µM and Nonidet P-40 (Amresco Inc, Solon, Ohio, USA) 0.1%. Optical density was read at 570/630 nm in an Infinite M200 TECAN, Austria. Benznidazole (Sigma Aldrich) was used as positive control and DMSO 1% as negative control. The compounds that reduced >45% of the parasite viability in the single-concentration screening were further assayed in the concentration range 3–100 µM for EC_{50} determination. For the assays where the parasites were treated with a combination of an active compound and benznidazole (1:1 ratio based on EC_{50}), the results were further analyzed in the software CompuSyn (ComboSyn, Inc) for calculation of combination indexes (CI) [72].

4.2.4. Cytotoxicity evaluation in THP-1 cells

THP-1 cells were grown and cultivated in 96 well plates (4.0×10^4 cells/well), as described in Section 4.2.3. The cells were treated with the compounds in the concentration range 15.6–500 µM and incubated for 72 h (37 °C, 5% CO_2). DMSO 1% was used as negative control, and DMSO 50% as positive control. Cell viability was assessed using the MTT assay. After the treatment time, 50 µL of 3-(4,5-dimethylthiazol-2-yl)-2,5-diphenyltetrazolium bromide (MTT, 3 mg/mL) was added to each well and the cells incubated for 4 h (37 °C, 5% CO_2). The culture medium was removed carefully, and the formazan crystals were dissolved with DMSO 100%. Immediately after, the optical density was read at 540 nm in an Infinite M200 TECAN microplate reader.

4.2.5. Haemolysis assay

180 µL of a 2% erythrocyte suspension (in NaCl 0.85% containing 10 nM of $CaCl_2$) was distributed in a 96 well-plate. The cells were treated with the test compounds to a final concentration of 100 and 50 µM and the plates were incubated under stirring for 4 h (37 °C). Then, the plates were centrifugated (3500 rpm, 5 min), the supernatant was carefully transferred to another 96 well-plate, and the absorbance at 540 nm was read in Infinite M200 TECAN microplate reader. Triton X-100 (1%) was used as positive control and DMSO 1% as negative control. The human cells used in this experiment were collected following a procedure approved by the Universidade Federal de Santa Catarina institutional review board for studies involving human subjects (Process 2190 FR 453659). All the procedures comply with national and international guidelines for the protection of human subjects from research-related risks.

4.2.6. Mithocondrial membrane potential assay in T. cruzi epimastigotes

Flow cytometry using rhodamine 123 (Rh-123) as probe was used for analyzing the mitochondrial membrane potential (ΔΨm) of *T. cruzi* epimastigotes after treatment. 1 mL of parasites (2.5 x 10^6 parasites/mL) was seeded in 48-well plates and treated with the active compounds in the final concentrations of EC_{50}, 2 x EC_{50}, 4 x EC_{50}, and 8 x ED_{50}. The parasites were maintained at 27 °C for 24 h and then centrifuged (3000 x g, 5 min) and washed with PBS. The parasites were incubated in PBS with 100 µL of R123 (5 µg/mL) for 20 min at 27 °C and then washed with PBS thrice again. The fluorescence of Rh-123 was measured in a FACSCalibur (BD Biosciences) (YAMANAKA et al., 2013). A total of 50.000 events were acquired in the region of light scattering (FSC x SSC) corresponding to the parasites. Relative mitochondrial membrane potential was determined by considering the fold change in the geometric mean of FL1-H signal intensity. The data were subsequently analyzed using the program FLOWJO (Treestar Software, Ashland, OR, USA). All experiments were performed in triplicate, using DMSO 1% as a negative control and pentamidine (100 µM) as positive control. Alterations in the fluorescence of Rh-123 were quantified using the ΔΨm index of variation (IV). The IV is calculated using the following equation:

$$\Delta\Psi\mathrm{m}\ IV = \frac{(MT - MC)}{MC}$$

Where MT and MC are the median of fluorescence for treated and negative control parasite, respectively. Negative IV values correspond to depolarization of the mitochondrial membrane [73].

4.2.7. Plasmatic membrane integrity assay in T. cruzi epimastigotes.

Flow cytometry using propidium iodide (PI) as probe was used for analyzing the plasmatic membrane integrity of *T. cruzi* epimastigotes after treatment. The experiment was conducted as described in Section 4.2.6. but the parasites were collected and incubated in PBS containing 100 µL of propidium iodide (10 µg/mL) instead. After 20 min, the parasites were washed with PBS thrice and quantified by flow cytometry as described above. The number of cells dyed by PI (PI+ cells) was expressed as percentage.

4.2.8. Trypanothione reductase inhibition assay

Recombinant trypanothione reductase from *T. cruzi* (TryR), was expressed in *Escherichia coli* (BL21DE3) and purified by affinity chromatography. TryR assays were performed as described by Hamilton et al. [74]. In 96 well micro plates (final volume = 240 µL), TryR (3.5 mU), HEPES (40 mM, pH 7.5), NADPH (0.15 mM), DTNB (25 µM) and EDTA (1 mM) were incubated for 5 min (27 "C) before trypanothione (1 mM) and the test compounds (100 µM) were added. Compounds and controls were pre-incubated at 27 °C for 30 min and 10 µL of DTNB was added to the reaction mixture. Absorbance at 412 nm was measured for 30 min in an Infinite M200 TECAN microplate reader to determine the enzymatic activity. DMSO 1% was used as negative control and clomipramine as positive control.

4.2.9. Statistical analysis

The EC_{50} and CC_{50} values were calculated from the non-linear regression of the dose-response curve using the software GraphPad Prism 9. One-way ANOVA followed by the post-hoc test Dunnet were used for comparing the means of treatment groups with the controls. The null hypothesis was rejected when $P < 0.05$.

References

[1] D. Steverding, The history of Chagas disease, Parasit. Vectors. 7 (2014) 317. https://doi.org/10.1186/1756-3305-7-317.

[2] M.C.P. Nunes, W. Dones, C.A. Morillo, J.J. Encina, A.L. Ribeiro, Chagas Disease, J. Am. Coll. Cardiol. 62 (2013) 767–776. https://doi.org/10.1016/j.jacc.2013.05.046.

[3] J.A. Pérez-Molina, I. Molina, Chagas disease, Lancet. 391 (2018) 82–94. https://doi.org/10.1016/S0140-6736(17)31612-4.

[4] S.L. James et al, Global, regional, and national incidence, prevalence, and years lived with disability for 354 diseases and injuries for 195 countries and territories, 1990–2017: a systematic analysis for the Global Burden of Disease Study 2017, Lancet. 392 (2018) 1789–1858. https://doi.org/10.1016/S0140-6736(18)32279-7.

[5] J. Altcheh, G. Moscatelli, S. Moroni, F. Garcia-Bournissen, H. Freilij, Adverse Events After the Use of Benznidazole in Infants and Children With Chagas Disease, Pediatrics. 127 (2011) e212–e218. https://doi.org/10.1542/peds.2010-1172.

[6] G.M. Sperandio da Silva, M.F. Felix Mediano, A.M. Hasslocher-Moreno, M.T. de Holanda, A. Silvestre de Sousa, L.H.C. Sangenis, P.E.A.A. do Brasil, R.A. Mejía, C.P. Fux, J.-C. Cubides, R.M. Saraiva, L.M. Brum-Soares, Benznidazole treatment safety: the Médecins Sans Frontières experience in a large cohort of Bolivian patients with Chagas' disease, J. Antimicrob. Chemother. 72 (2017) 2596–2601. https://doi.org/10.1093/jac/dkx180.

[7] Y. Jackson, E. Alirol, L. Getaz, H. Wolff, C. Combescure, F. Chappuis, Tolerance and Safety of Nifurtimox in Patients with Chronic Chagas Disease, Clin. Infect. Dis. 51 (2010) e69–e75. https://doi.org/10.1086/656917.

[8] V. de S. Fernandes, R. Rosa, L.A. Zimmermann, K.R. Rogério, A.E. Kümmerle, L.S.C. Bernardes, C.S. Graebin, Antiprotozoal agents: How have they changed over a decade?, Arch. Pharm. (Weinheim). (2021) e2100338. https://doi.org/10.1002/ardp.202100338.

[9] L.S. Filardi, Z. Brener, Susceptibility and natural resistance of Trypanosoma cruzi strains to drugs used clinically in Chagas disease, Trans. R. Soc. Trop. Med. Hyg. 81 (1987) 755–759. https://doi.org/10.1016/0035-9203(87)90020-4.

[10] H.M. Andrade, S.M.F. Murta, A. Chapeaurouge, J. Perales, P. Nirdé, A.J. Romanha, Proteomic Analysis of Trypanosoma cruzi Resistance to Benznidazole, J. Proteome Res. 7 (2008) 2357–2367. https://doi.org/10.1021/pr700659m.

[11] C.A. Morillo, J.A. Marin-Neto, A. Avezum, S. Sosa-Estani, A. Rassi, F. Rosas, E. Villena, R. Quiroz, R. Bonilla, C. Britto, F. Guhl, E. Velazquez, L. Bonilla, B. Meeks, P. Rao-Melacini, J. Pogue, A. Mattos, J. Lazdins, A. Rassi, S.J. Connolly, S. Yusuf, Randomized Trial of Benznidazole for Chronic Chagas' Cardiomyopathy, N. Engl. J. Med. 373 (2015) 1295–1306. https://doi.org/10.1056/NEJMoa1507574.

[12] C.A. Morillo, H. Waskin, S. Sosa-Estani, M. del Carmen Bangher, C.A.C. Cuneo, R.R.R. Milesi, M.M.H. Mallagray, W. Apt, J.S.J. Beloscar, J. Gascon, I. Molina, L.E. Echeverria, H. Colombo, J.A.J.A. Perez-Molina, F.F.S. Wyss, B. Meeks, L.R. Bonilla, P. Gao, B. Wei, M. McCarthy, S. Yusuf, C.A. Morillo, S. Sosa-Estani, H. Waskin, B. Meeks, S. Yusuf, R. Diaz, H. Acquatella, J. Lazzari, R. Roberts, M. Traina, B. Meeks, L.R. Bonilla, P. Gao, A. Taylor, I. Holadyk-Gris, L. Whalen, M.C. Bangher, M.A. Romero, N. Prado, Y. Hernández, M. Fernandez, A. Riarte, K. Scollo, C. Lopez-Albizu, C.A.C. Cuneo, N.C. Gutiérrez, R.R.R. Milesi, M.A. Berli, M.M.H. Mallagray, N.E. Cáceres, J.S.J. Beloscar, J.M. Petrucci, H. Colombo, M. Dellatorre, A. Prado, W. Apt, I. Zulantay, L.E. Echeverría, D. Isaza, E. Reyes, F.F.S. Wyss, A. Figueroa, I. Guzmán Melgar, E. Rodríguez, J. Gascon, E. Aldasoro, E.J. Posada, N. Serret, I. Molina, A. Sánchez-Montalvá, J.A.J.A. Perez-Molina, R. López-Vélez, P.A. Reyes-López, Benznidazole and Posaconazole in Eliminating Parasites in Asymptomatic T. Cruzi Carriers, J. Am. Coll. Cardiol. 69 (2017) 939–947. https://doi.org/10.1016/j.jacc.2016.12.023.

[13] J.A. Urbina, G. Payares, C. Sanoja, R. Lira, A.J. Romanha, In vitro and in vivo activities of ravuconazole on Trypanosoma cruzi, the causative agent of Chagas disease, Int. J. Antimicrob. Agents. 21 (2003) 27–38. https://doi.org/10.1016/S0924-8579(02)00273-X.

[14] L. d. F. Diniz, I.S. Caldas, P.M. d. M. Guedes, G. Crepalde, M. de Lana, C.M. Carneiro, A. Talvani, J.A. Urbina, M.T. Bahia, Effects of Ravuconazole Treatment on Parasite Load and Immune Response in Dogs Experimentally Infected with Trypanosoma cruzi, Antimicrob. Agents Chemother. 54 (2010) 2979–2986. https://doi.org/10.1128/AAC.01742-09.

[15] F. Torrico, J. Gascon, L. Ortiz, C. Alonso-Vega, M.-J. Pinazo, A. Schijman, I.C. Almeida, F. Alves, N. Strub-Wourgaft, I. Ribeiro, G. Santina, B. Blum, E. Correia, F. Garcia-Bournisen, M. Vaillant, J.R. Morales, J.J. Pinto Rocha, G. Rojas Delgadillo, H.R. Magne Anzoleaga, N. Mendoza, R.C. Quechover, M.Y.E. Caballero, D.F. Lozano Beltran, A.M. Zalabar, L. Rojas Panozo, A. Palacios Lopez, D. Torrico Terceros, V.A. Fernandez Galvez, L. Cardozo, G. Cuellar, R.N. Vasco Arenas, I. Gonzales, C.F. Hoyos Delfin, L. Garcia, R. Parrado, A. de la Barra, N. Montano, S. Villarroel, T. Duffy, M. Bisio, J.C. Ramirez, F. Duncanson, M. Everson, A. Daniels, M. Asada, E. Cox, D. Wesche, P.M. Diderichsen, A.F. Marques, L. Izquierdo, S.S. Sender, J.C. Reverter, M. Morales, W. Jimenez, Treatment of adult chronic indeterminate Chagas disease with benznidazole and three E1224 dosing regimens: a proof-of-concept, randomised, placebo-controlled trial, Lancet Infect. Dis. 18 (2018) 419–430. https://doi.org/10.1016/S1473-3099(17)30538-8.

[16] V.K.B.K. Mesu, W.M. Kalonji, C. Bardonneau, O.V. Mordt, S. Blesson, F. Simon, S. Delhomme, S. Bernhard, W. Kuziena, J.-P.F. Lubaki, S.L. Vuvu, P.N. Ngima, H.M. Mbembo, M. Ilunga, A.K. Bonama, J.A. Heradi, J.L.L. Solomo, G. Mandula, L.K. Badibabi, F.R. Dama, P.K. Lukula, D.N. Tete, C. Lumbala, B. Scherrer, N. Strub-Wourgaft, A. Tarral, Oral fexinidazole for late-stage African Trypanosoma brucei gambiense trypanosomiasis: a pivotal multicentre, randomised, non-inferiority trial, Lancet. 391 (2018) 144–154. https://doi.org/10.1016/S0140-6736(17)32758-7.

[17] M.T. Bahia, A.F.S. Nascimento, A.L. Mazzeti, L.F. Marques, K.R. Gonçalves, L.W.R. Mota, L.F. De Diniz, I.S. Caldas, A. Talvani, D.M. Shackleford, M. Koltun, J. Saunders, K.L. White, I. Scandale, S.A. Charman, E. Chatelain, Antitrypanosomal activity of fexinidazole metabolites, potential new drug candidates for Chagas disease, Antimicrob. Agents Chemother. 58 (2014)

4362–4370. https://doi.org/10.1128/AAC.02754-13.
[18] B. David, J.-L. Wolfender, D.A. Dias, The pharmaceutical industry and natural products: historical status and new trends, Phytochem. Rev. 14 (2015) 299–315. https://doi.org/10.1007/s11101-014-9367-z.
[19] B. Shen, A New Golden Age of Natural Products Drug Discovery, Cell. 163 (2015) 1297–1300. https://doi.org/10.1016/j.cell.2015.11.031.
[20] H. Yuan, Q. Ma, L. Ye, G. Piao, The Traditional Medicine and Modern Medicine from Natural Products, Molecules. 21 (2016) 559. https://doi.org/10.3390/molecules21050559.
[21] J. Dai, R. Han, Y. Xu, N. Li, J. Wang, W. Dan, Recent progress of antibacterial natural products: Future antibiotics candidates, Bioorg. Chem. 101 (2020) 103922. https://doi.org/10.1016/j.bioorg.2020.103922.
[22] E. Izumi, T. Ueda-Nakamura, B.P. Dias Filho, V.F. Veiga Júnior, C.V. Nakamura, Natural products and Chagas' disease: a review of plant compounds studied for activity against Trypanosoma cruzi., Nat. Prod. Rep. 28 (2011) 809–823. https://doi.org/10.1039/c0np00069h.
[23] A.G. Atanasov, B. Waltenberger, E.-M. Pferschy-Wenzig, T. Linder, C. Wawrosch, P. Uhrin, V. Temml, L. Wang, S. Schwaiger, E.H. Heiss, J.M. Rollinger, D. Schuster, J.M. Breuss, V. Bochkov, M.D. Mihovilovic, B. Kopp, R. Bauer, V.M. Dirsch, H. Stuppner, Discovery and resupply of pharmacologically active plant-derived natural products: A review, Biotechnol. Adv. 33 (2015) 1582–1614. https://doi.org/10.1016/j.biotechadv.2015.08.001.
[24] A.G. Atanasov, S.B. Zotchev, V.M. Dirsch, C.T. Supuran, Natural products in drug discovery: advances and opportunities, Nat. Rev. Drug Discov. 20 (2021) 200–216. https://doi.org/10.1038/s41573-020-00114-z.
[25] H. Wahyudi, S.R. McAlpine, Predicting the unpredictable: Recent structure–activity studies on peptide-based macrocycles, Bioorg. Chem. 60 (2015) 74–97. https://doi.org/10.1016/j.bioorg.2015.04.009.
[26] S.N.A. Bukhari, G.B. Kumar, H.M. Revankar, H.-L. Qin, Development of combretastatins as potent tubulin polymerization inhibitors., Bioorg. Chem. 72 (2017) 130–147. https://doi.org/10.1016/j.bioorg.2017.04.007.
[27] D.J. Newman, G.M. Cragg, Natural Products as Sources of New Drugs over the Nearly Four Decades from 01/1981 to 09/2019, J. Nat. Prod. 83 (2020) 770–803. https://doi.org/10.1021/acs.jnatprod.9b01285.
[28] R. da Rosa, E.P. Schenkel, L.S.C. Bernardes, Semisynthetic and newly designed derivatives based on natural chemical scaffolds: moving beyond natural products to fight Trypanosoma cruzi, Phytochem. Rev. (2020). https://doi.org/10.1007/s11101-020-09659-8.
[29] M.T. Varela, T.A. Costa-Silva, J.H.G. Lago, A.G. Tempone, J.P.S. Fernandes, Evaluation of the antitrypanosoma activity and SAR study of novel LINS03 derivatives, Bioorg. Chem. 89 (2019) 102996. https://doi.org/10.1016/j.bioorg.2019.102996.
[30] R.B. Teponno, S. Kusari, M. Spiteller, Recent advances in research on lignans and neolignans, Nat. Prod. Rep. 33 (2016) 1044–1092. https://doi.org/10.1039/C6NP00021E.
[31] A.A. da Silva Filho, S. Albuquerque, M.L.A. e Silva, M.N. Eberlin, D.M. Tomazela, J.K. Bastos, Tetrahydrofuran Lignans from Nectandra m egapotamica with Trypanocidal Activity ⊥, J. Nat. Prod. 67 (2004) 42–45. https://doi.org/10.1021/np0302697.
[32] L.G. Felippe, D.C. Baldoqui, M.J. Kato, V. da S. Bolzani, E.F. Guimarães, R.M.B. Cicarelli, M. Furlan, Trypanocidal tetrahydrofuran lignans from Peperomia blanda, Phytochemistry. 69 (2008) 445–450. https://doi.org/10.1016/j.phytochem.2007.08.012.
[33] N.P. Lopes, P. Chicaro, M.J. Kato, S. Albuquerque, M. Yoshida, Flavonoids and Lignans from Virola surinamensis Twigs and their in vitro Activity against Trypanosoma cruzi, Planta Med. 64 (1998) 667–669.
[34] K. Matcha, S. Ghosh, An asymmetric route to total synthesis of the furano lignan (+)-veraguensin, Tetrahedron Lett. 51 (2010) 6924–6927. https://doi.org/10.1016/j.tetlet.2010.10.136.
[35] R. Stevenson, J.H. Williams, Synthesis of tetrahydrofuran lignans, (±)-galbelgin and (±)-grandisin, Tetrahedron. 33 (1977) 285–288. https://doi.org/10.1016/0040-4020(77)80107-5.
[36] C.E. Rye, D. Barker, Asymmetric Synthesis of (+)-Galbelgin, (-)-Kadangustin J, (-)-Cyclogalgravin and (-)-Pycnanthulignenes A and B , Three Structurally Distinct Lignan Classes , Using a Common Chiral Precursor, J. Org. Chem. 76 (2011) 6636–6648. https://doi.org/10.1021/jo200968f.
[37] K. Nihei, Synthesis of trypanocidal tetrahydrofuran lignans, Arkivoc. 2004 (2004) 112–126. https://doi.org/10.3998/ark.5550190.0005.615.
[38] L.S.C. Bernardes, M.J. Kato, S. Albuquerque, I. Carvalho, Synthesis and trypanocidal activity of

1,4-bis-(3,4,5-trimethoxy-phenyl)-1,4-butanediol and 1,4-bis-(3,4-dimethoxyphenyl)-1,4-butanediol, Bioorganic Med. Chem. 14 (2006) 7075–7082. https://doi.org/10.1016/j.bmc.2006.07.006.

[39] A.P. Hartmann, M.R. de Carvalho, L.S.C. Bernardes, M.H.M.H. de Moraes, E.B. de Melo, M. Steindel, J.S. Silva, I. Carvalho, M.R. de Carvalho, L.S.C. Bernardes, M.H. de Moraes, E.B. de Melo, C.D. Lopes, M. Steindel, J.S. da Silva, I. Carvalho, M.H.M.H. de Moraes, E.B. de Melo, C.D. Lopes, M. Steindel, J.S. da Silva, I. Carvalho, Synthesis and 2D-QSAR studies of neolignan-based diaryl-tetrahydrofuran and -furan analogues with remarkable activity against Trypanosoma cruzi and assessment of the trypanothione reductase activity, Eur. J. Med. Chem. 140 (2017) 187–199. https://doi.org/10.1016/j.ejmech.2017.08.064.

[40] R. da Rosa, M.H. de Moraes, L.A. Zimmermann, E.P. Schenkel, M. Steindel, L.S.C. Bernardes, Design and synthesis of a new series of 3,5-disubstituted isoxazoles active against Trypanosoma cruzi and Leishmania amazonensis, Eur. J. Med. Chem. 128 (2017) 25–35. https://doi.org/10.1016/j.ejmech.2017.01.029.

[41] T.B. Cassamale, E.C. Costa, D.B. Carvalho, N.S. Cassemiro, C.C. Tomazela, M.C.S. Marques, M. Ojeda, M.F.C. Matos, S. Albuquerque, C.C.P. Arruda, A.C.M. Baroni, Synthesis and Antitrypanosomastid Activity of 1,4-Diaryl-1,2,3-triazole Analogues of Neolignans Veraguensin, Grandisin and Machilin G, J. Braz. Chem. Soc. 27 (2016) 1217–1228. https://doi.org/10.5935/0103-5053.20160017.

[42] L.A. Zimmermann, M.H. de Moraes, R. da Rosa, E.B. de Melo, F.R. Paula, E.P. Schenkel, M. Steindel, L.S.C. Bernardes, Synthesis and SAR of new isoxazole-triazole bis-heterocyclic compounds as analogues of natural lignans with antiparasitic activity, Bioorg. Med. Chem. 26 (2018) 4850–4862. https://doi.org/10.1016/j.bmc.2018.08.025.

[43] J. Ziegler, P.J. Facchini, Alkaloid Biosynthesis: Metabolism and Trafficking, Annu. Rev. Plant Biol. 59 (2008) 735–769. https://doi.org/10.1146/annurev.arplant.59.032607.092730.

[44] B.R. Lichman, The scaffold-forming steps of plant alkaloid biosynthesis, Nat. Prod. Rep. 38 (2021) 103–129. https://doi.org/10.1039/D0NP00031K.

[45] W. Crow, J. Hodgkin, Alkaloids of the Australian Rutaceae: Halfordia scleroxyla. II. Isolation and structure of the alkaloids, Aust. J. Chem. 17 (1964) 119. https://doi.org/10.1071/CH9640119.

[46] B. A. Burke, B. Burke, H. Parkins, A. Marie Talbot, An Oxazole and Its Precursor in Amyris balsamifera, Heterocycles. 12 (1979) 349. https://doi.org/10.3987/R-1979-03-0349.

[47] G. de la Fuente, X. A. Dom地guez, A. G. Gonz◆ez. Mat痴 Reina, I. Tim溶, Two New Oxazoles from Amyris texana P. Wilson, Heterocycles. 27 (1988) 35. https://doi.org/10.3987/COM-87-4326.

[48] A.C. Giddens, H.I.M. Boshoff, S.G. Franzblau, C.E. Barry, B.R. Copp, Antimycobacterial natural products: synthesis and preliminary biological evaluation of the oxazole-containing alkaloid texaline, Tetrahedron Lett. 46 (2005) 7355–7357. https://doi.org/10.1016/j.tetlet.2005.08.119.

[49] N. Rastogi, Antimycobacterial activity of chemically defined natural substances from the Caribbean flora in Guadeloupe, FEMS Immunol. Med. Microbiol. 20 (1998) 267–273. https://doi.org/10.1016/S0928-8244(98)00021-2.

[50] A. Karmase, R. Birari, K.K. Bhutani, Evaluation of anti-obesity effect of Aegle marmelos leaves, Phytomedicine. 20 (2013) 805–812. https://doi.org/10.1016/j.phymed.2013.03.014.

[51] O. Banzragchgarav, T. Murata, G. Odontuya, B. Buyankhishig, K. Suganuma, B.-O. Davaapurev, N. Inoue, J. Batkhuu, K. Sasaki, Trypanocidal Activity of 2,5-Diphenyloxazoles Isolated from the Roots of Oxytropis lanata, J. Nat. Prod. 79 (2016) 2933–2940. https://doi.org/10.1021/acs.jnatprod.6b00778.

[52] A.J. Robles, S. McCowen, S. Cai, M. Glassman, F. Ruiz, R.H. Cichewicz, S.F. McHardy, S.L. Mooberry, Structure–Activity Relationships of New Natural Product-Based Diaryloxazoles with Selective Activity against Androgen Receptor-Positive Breast Cancer Cells, J. Med. Chem. 60 (2017) 9275–9289. https://doi.org/10.1021/acs.jmedchem.7b01228.

[53] D. Yamamuro, R. Uchida, M. Ohtawa, S. Arima, Y. Futamura, M. Katane, H. Homma, T. Nagamitsu, H. Osada, H. Tomoda, Synthesis and biological activity of 5-(4-methoxyphenyl)-oxazole derivatives, Bioorg. Med. Chem. Lett. 25 (2015) 313–316. https://doi.org/10.1016/j.bmcl.2014.11.042.

[54] K. Narita, K. Suganuma, T. Murata, R. Kondo, H. Satoh, K. Watanabe, K. Sasaki, N. Inoue, Y. Yoshimura, Synthesis and evaluation of trypanocidal activity of derivatives of naturally occurring 2,5-diphenyloxazoles, Bioorg. Med. Chem. 42 (2021) 116253. https://doi.org/10.1016/j.bmc.2021.116253.

[55] W. Fan, C. Verrier, Y. Queneau, F. Popowycz, 5-Hydroxymethylfurfural (HMF) in Organic Synthesis: A Review of its Recent Applications Towards Fine Chemicals, Curr. Org. Synth. 16

(2019) 583–614. https://doi.org/10.2174/1570179416666190412164738.
[56] A.A. Rosatella, S.P. Simeonov, R.F.M. Frade, C.A.M. Afonso, 5-Hydroxymethylfurfural (HMF) as a building block platform: Biological properties, synthesis and synthetic applications, Green Chem. 13 (2011) 754. https://doi.org/10.1039/c0gc00401d.
[57] R. da Rosa, L. Grand, E.P. Schenkel, L. Sibelle Campos Bernardes, M. Jacolot, F. Popowycz, The Use of 5-Hydroxymethylfurfural towards Fine Chemicals: Synthesis and Direct Arylation of 5-HMF-Based Oxazoles, Synlett. 32 (2021) 838–844. https://doi.org/10.1055/a-1335-7330.
[58] T.-C. Chou, Theoretical Basis, Experimental Design, and Computerized Simulation of Synergism and Antagonism in Drug Combination Studies, Pharmacol. Rev. 58 (2006) 621–681. https://doi.org/10.1124/pr.58.3.10.
[59] J. Meletiadis, T. Stergiopoulou, E.M. O'Shaughnessy, J. Peter, T.J. Walsh, Concentration-Dependent Synergy and Antagonism within a Triple Antifungal Drug Combination against Aspergillus Species: Analysis by a New Response Surface Model, Antimicrob. Agents Chemother. 51 (2007) 2053–2064. https://doi.org/10.1128/AAC.00873-06.
[60] A.M. Tomás, H. Castro, Redox Metabolism in Mitochondria of Trypanosomatids, Antioxid. Redox Signal. 19 (2013) 696–707. https://doi.org/10.1089/ars.2012.4948.
[61] P.S. Brookes, Y. Yoon, J.L. Robotham, M.W. Anders, S.-S. Sheu, Calcium, ATP, and ROS: a mitochondrial love-hate triangle, Am. J. Physiol. Physiol. 287 (2004) C817–C833. https://doi.org/10.1152/ajpcell.00139.2004.
[62] L.M. Fidalgo, L. Gille, Mitochondria and Trypanosomatids: Targets and Drugs, Pharm. Res. 28 (2011) 2758–2770. https://doi.org/10.1007/s11095-011-0586-3.
[63] M. Huang, A.K.S. Camara, D.F. Stowe, F. Qi, D.A. Beard, Mitochondrial Inner Membrane Electrophysiology Assessed by Rhodamine-123 Transport and Fluorescence, Ann. Biomed. Eng. 35 (2007) 1276–1285. https://doi.org/10.1007/s10439-007-9265-2.
[64] B. Manta, M. Comini, A. Medeiros, M. Hugo, M. Trujillo, R. Radi, Trypanothione: A unique bis-glutathionyl derivative in trypanosomatids, Biochim. Biophys. Acta - Gen. Subj. 1830 (2013) 3199–3216. https://doi.org/10.1016/j.bbagen.2013.01.013.
[65] T. Battista, G. Colotti, A. Ilari, A. Fiorillo, Targeting Trypanothione Reductase, a Key Enzyme in the Redox Trypanosomatid Metabolism, to Develop New Drugs against Leishmaniasis and Trypanosomiases, Molecules. 25 (2020) 1924. https://doi.org/10.3390/molecules25081924.
[66] A.A.S. Mendonça, C.M. Coelho, M.P. Veloso, I.S. Caldas, R.V. Gonçalves, A.L. Teixeira, A.S. de Miranda, R.D. Novaes, Relevance of Trypanothione Reductase Inhibitors on Trypanosoma cruzi Infection: A Systematic Review, Meta-Analysis, and In Silico Integrated Approach, Oxid. Med. Cell. Longev. 2018 (2018) 1–20. https://doi.org/10.1155/2018/8676578.
[67] C.A. Lipinski, Drug-like properties and the causes of poor solubility and poor permeability, J. Pharmacol. Toxicol. Methods. 44 (2000) 235–249. https://doi.org/10.1016/S1056-8719(00)00107-6.
[68] S. Tian, J. Wang, Y. Li, D. Li, L. Xu, T. Hou, The application of in silico drug-likeness predictions in pharmaceutical research, Adv. Drug Deliv. Rev. 86 (2015) 2–10. https://doi.org/10.1016/j.addr.2015.01.009.
[69] E.A.G. Blomme, Y. Will, Toxicology Strategies for Drug Discovery: Present and Future, Chem. Res. Toxicol. 29 (2016) 473–504. https://doi.org/10.1021/acs.chemrestox.5b00407.
[70] I. Peña, M. Pilar Manzano, J. Cantizani, A. Kessler, J. Alonso-Padilla, A.I. Bardera, E. Alvarez, G. Colmenarejo, I. Cotillo, I. Roquero, F. de Dios-Anton, V. Barroso, A. Rodriguez, D.W. Gray, M. Navarro, V. Kumar, A. Sherstnev, D.H. Drewry, J.R. Brown, J.M. Fiandor, J. Julio Martin, New Compound Sets Identified from High Throughput Phenotypic Screening Against Three Kinetoplastid Parasites: An Open Resource, Sci. Rep. 5 (2015) 8771. https://doi.org/10.1038/srep08771.
[71] T. Sander, J. Freyss, M. von Korff, C. Rufener, DataWarrior: An Open-Source Program For Chemistry Aware Data Visualization And Analysis, J. Chem. Inf. Model. 55 (2015) 460–473. https://doi.org/10.1021/ci500588j.
[72] T.-C. Chou, Drug Combination Studies and Their Synergy Quantification Using the Chou-Talalay Method, Cancer Res. 70 (2010) 440–446. https://doi.org/10.1158/0008-5472.CAN-09-1947.
[73] R.F.S. Menna-Barreto, R.L.S. Goncalves, E.M. Costa, R.S.F. Silva, A. V. Pinto, M.F. Oliveira, S.L. de Castro, The effects on Trypanosoma cruzi of novel synthetic naphthoquinones are mediated by mitochondrial dysfunction, Free Radic. Biol. Med. 47 (2009) 644–653. https://doi.org/10.1016/J.FREERADBIOMED.2009.06.004.
[74] C.J. Hamilton, A. Saravanamuthu, I.M. Eggleston, A.H. Fairlamb, Ellman's-reagent-mediated regeneration of trypanothione in situ: substrate-economical microplate and time-dependent inhibition assays for trypanothione reductase., Biochem. J. 369 (2003) 529–537.

https://doi.org/10.1042/BJ20021298.

Natural chemical scaffolds

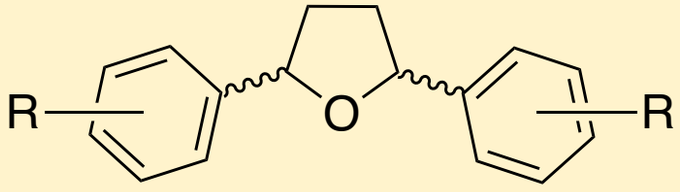

Tetrahydrofuran lignans

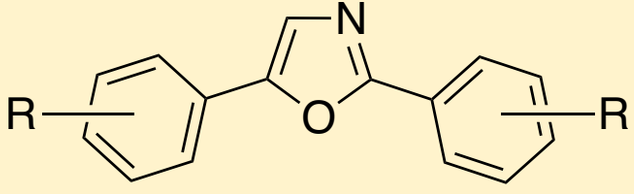

Oxazole alkaloids

Design and synthesis of analogs

In vitro biological evaluation against *T. cruzi*

SAR, toxicity and MoA investigation

Forty-six synthetic analogs

5-membered heterocycles and polar acyclic linkers

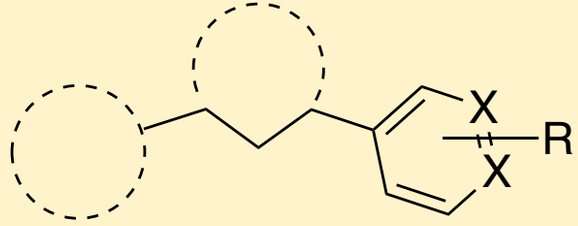

1,3-benzodioxol-5-yl or 5-hydroxymethylfur-2-yl

X = *C or N*
R = *alkyl, aryl, EDG or EWG*

Evaluation of selectivity, hemocompatibility, trypanothione reductase inhibition, mitochondrial effects, and synergistic potential.